NUMERICAL ANALYSIS OF REINFORCED CONCRETE BEAM COLUMN JOINT RETROFITTED USING CARBON FIBER REINFORCED POLYMER (CFRP) SHEETS

PROJECT REPORT

Submitted by

SEENA JALAL

TKM20CESC13

to

the A P J Abdul Kalam Technological University

in partial fulfillment of the requirements for the award of the Degree

of

Master of Technology

in

Structural Engineering & Construction Management

Department of Civil Engineering

TKM College of Engineering, Kollam-691005

July 2022

DECLARATION

I undersigned hereby declare that the project report "Numerical Analysis of Reinforced Concrete Beam Column Joint Retrofitted using Carbon Fiber Reinforced Polymer (CFRP) Sheets", submitted for partial fulfillment of the requirements for the award of degree of Master of Technology of the APJ Abdul Kalam Technological University, Kerala is a bonafide work done by me under supervision of Prof. Rekha Ambi, Assistant Professor, Department of Civil Engineering. This submission represents my ideas in my own words and where ideas or words of others have been included. I have adequately and accurately cited and referenced the original sources. I also declare that I have adhered to ethics of academic honesty and integrity and have not misrepresented or fabricated any data or idea or fact or source in my submission. I understand that any violation of the above will be a cause for disciplinary action by the institute and or the University and can also evoke penal action from the sources which have thus not been properly cited or from whom proper permission has not been obtained. This report has not been previously formed the basis for the award of any degree, diploma or similar title of any other University.

Kollam

06/07/2022 **SEENA JALAL**

DEPARTMENT OF CIVIL ENGINEERING

T.K.M. College of Engineering, Kollam

CERTIFICATE

Certified that this report entitled **'NUMERICAL ANALYSIS OF REINFORCED CONCRETE BEAM COLUMN JOINT RETROFITTED USING CARBON FIBER REINFORCED POLYMER (CFRP) SHEETS'** is the report of project presented by **SEENA JALAL, Roll No: M20CESC13** during **2020-2022** in partial fulfillment of the requirements for the award of the Degree of Master of Technology in Structural Engineering & Construction Management of the A P J Abdul Kalam Technological University.

Guide	Coordinator	Head of the Department
Prof. REKHA AMBI	**Dr. RAMASWAMY K.P.**	**Dr. SAJEEB R.**
Assistant Professor,	Assistant Professor,	Professor,
Dept. of Civil Engg.,	Dept. of Civil Engg.,	Dept. of Civil Engg.,
TKMCE, Kollam.	TKMCE, Kollam.	TKMCE, Kollam.

ACKNOWLEDGEMENT

I take this opportunity to express my deep sense of gratitude and sincere thanks to all who helped me to complete the project successfully.

I am deeply indebted to my guide, **Prof. Rekha Ambi**, Assistant Professor, Department of Civil Engineering for her excellent guidance, positive criticism and valuable comments.

I am greatly thankful to my project coordinator, Dr. **Ramaswamy K.P.,** Assistant Professor, Department of Civil Engineering for his constant supervision as well as for providing necessary information regarding the project.

I am greatly thankful to **Dr. Sajeeb R.**, Professor and Head of the Department of Civil Engineering, for his kind support.

Finally, I thank my parents and friends who directly and indirectly contributed to the successful completion of my project.

Above all, I thank the almighty God for the successful conduct of this project.

SEENA JALAL

ABSTRACT

The beam column joint is the critical zone in a reinforced cement concrete (RCC) moment resisting frame. It is subjected to large forces during severe ground shaking and its behavior has a significant influence on the response of a structure. Improper design and detailing of joint will result in brittle failures. To avoid such failures and meet specific beam column joint requirements, existing reinforced concrete structures must be strengthened. Retrofitting and strengthening are the most sustainable methods for improving the performance of reinforced concrete frame buildings. There are several methods for retrofitting beam column joints, the most common of which is Carbon Fiber Reinforced Polymer (CFRP). CFRP is a popular material for retrofitting due to its superior properties such as high corrosion resistance, high strength, high stiffness, and good resistance to chemical attack etc. Thus, it is important to examine more about retrofitting using carbon fiber reinforced polymer.

This thesis paper is set out to study and provide insights about what is retrofitting, importance of retrofitting a beam column joint, and effectiveness of using of CFRP as a retrofitting agent for beam column joint based on numerical analysis.

In this study, reinforced beam column joint retrofitted using CFRP is considered. Numerical investigation is done on normal beam column joint and CFRP retrofitted beam column joint. The numerical investigation is done using ABAQUS software. This study focuses on the influence of the orientation and number of layers of CFRP sheet with different fiber orientation on the performance of retrofitted joint. The comparison of the performance of retrofitted joint models in terms of load carrying capacity, ductility, energy dissipation capacity and stiffness degradation were also studied.

Keywords: *Reinforced Cement Concrete (RCC) structures, Beam Column Joint, Retrofitting, Carbon Fiber Reinforced Polymer (CFRP), Abaqus.*

CONTENTS

LIST OF FIGURES

LIST OF TABLES

ABBREVIATIONS

AFRP	Aramid Fiber Reinforced Polymer
BFRP	Basalt Fiber Reinforced Polymer
B-C	Beam-Column
C3D8R	3d 8-Noded Hexahedral Elements
CDP	Concrete Damage Plasticity
CFRP	Carbon Fiber Reinforced Polymer
EBR	Externally Bonded Reinforcement
EBROG	Externally Bonded Reinforcement on Grooves
EBRIG	Externally Bonded Reinforcement in Grooves
FEA	Finite Element Analysis
FRP	Fiber-Reinforced Polymer
GFRP	Glass Fiber-Reinforced Polymer
GM	Grooving Method
NSM	Near-Surface Mounted
RCC	Reinforced Cement Concrete ()
S4R	4-Noded Shell Element
T3D2	2-Noded Truss Elements
UHP-HFRC	Ultrahigh-Performance Hybrid Fiber Reinforced Concrete

CHAPTER 1
INTRODUCTION

1.1 GENERAL

Reinforced Cement Concrete (RCC) structures are frequently found to be distressed and damaged even before their service life is over due to various reasons such as earthquakes, corrosion, overloading, improper design, faulty construction, explosions, and fire. Beam-column joints are critical areas in the analysis and design of moment-resisting reinforced concrete frames. The design check for beam column joints is not generally considered in normal design practice. As a result, the joint design is not always done properly. However, during earthquakes, the failure of reinforced concrete frames has demonstrated significant distress due to shear failure of beam column joint, resulting in the structural collapse. Shear failure is not an acceptable structural performance. The building should be designed and detailed properly to provide adequate strength and ductility to withstand large deformations caused by earthquakes. In most cases, the cost of replacing a deficient structure exceeds the cost of strengthening. As a result, strengthening and retrofitting techniques are widely used to increase a structure's load carrying capacity. The process of increasing a building's seismic resistance is known as retrofitting. The need for retrofitting is growing by the day due to a variety of factors such as increased seismic activity, natural disasters, increased live loads on existing structures, and so on. Some of the most commonly used retrofitting techniques are ferrocement jacketing, epoxy injection, shear wall addition, fiber reinforced polymer etc. Carbon Fiber Reinforced Polymer (CFRP) is an effective retrofitting material due to its light weight, high strength, and corrosion resistance. The behavior of a structure is determined by the nature of the beam-column joint, so strengthening of beam-column joint is critical. Joints sustain serious damage during earthquakes when large forces are present. Unsafe design and detailing of joint are dangerous and it will jeopardize the structure. Researchers and engineers have been inspired to use polymer composites in the field of structural rehabilitation by the superior characteristics of (FRP) polymer composite materials, such as high corrosion resistance, high strength, high stiffness, excellent fatigue performance, and good resistance to chemical attack, among others. Retrofitting and strengthening are the most environmentally friendly and efficient ways to improve the performance of a beam

column joint. Existing reinforced concrete structures need to be strengthened in order to meet specific standards and safety requirements.

1.2 BEAM COLUMN JOINT

The beam column joint is defined as the portion of the column that frames into the column within the depth of the deepest beam. The joints should be strong and stiff enough to withstand the internal forces induced by the framing members. The zone where beams and columns connect is where a joint's functional need is to permit adjacent members to develop and sustain their maximum capacity (Alsayed et al., 2010). The beam column joint is the most important part of all framed structures, and the structural design of the joint is neglected during the design stage, with attention only limited to providing sufficient anchorage for the beam. Even if the structural elements themselves meet the design criteria, unsafe joint design and details pose a threat to the entire structure (Kadarningsih et al., 2014). It is well understood that the joint region in reinforced concrete framed structures is extremely important because it transfers forces and bending moments between the beams and columns. If the beam column joints are not adequately built, they are typically the most vulnerable part during heavy loading. There are three types of joints in a moment resisting frame: interior joint, exterior joint, and corner joint (Uma and Prasad, 2015). Figure 1.1(a) depicts an interior joint formed by four beams framing into the vertical faces of a column. The joint is known as an external joint when one beam frames into the vertical face of the column and two other beams frame into the joint from perpendicular directions. A typical exterior joint is depicted in figure 1.1(b). When two beam frames are joined into two adjacent vertical faces of a column, the joint is known as a corner joint, as illustrated in figure 1.1(c).

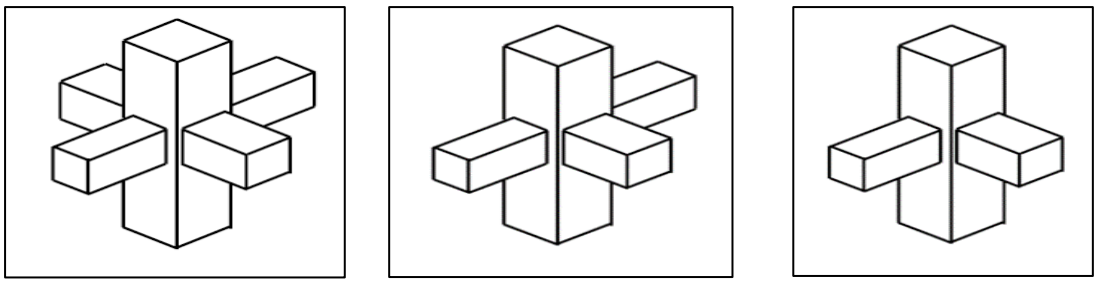

(a) Interior joint (b) Exterior joint (c) Corner joint

Figure 1.1 Types of joints in a frame: (a) Interior joint, (b) Exterior joint and (c) Corner joint

(Source: Uma and Prasad, 2015)

The severity of the forces and moments acting on the frame determines the performance of these joints and hence necessitates a better understanding of their seismic behaviour. Within the joint, these forces generate complex mechanisms involving bond and shear. Figure 1.2 shows a typical frame with exterior, interior, and corner joints. Beams are expected to form plastic hinges at their ends and develop flexural overstrength beyond the design strength in the strong column-weak beam design (Patil et al., 2013). The joint behaviour is characterized by a complex interaction between bond and shear. The bond performance of the bars anchored in a joint has a significant impact on the shear resisting mechanism.

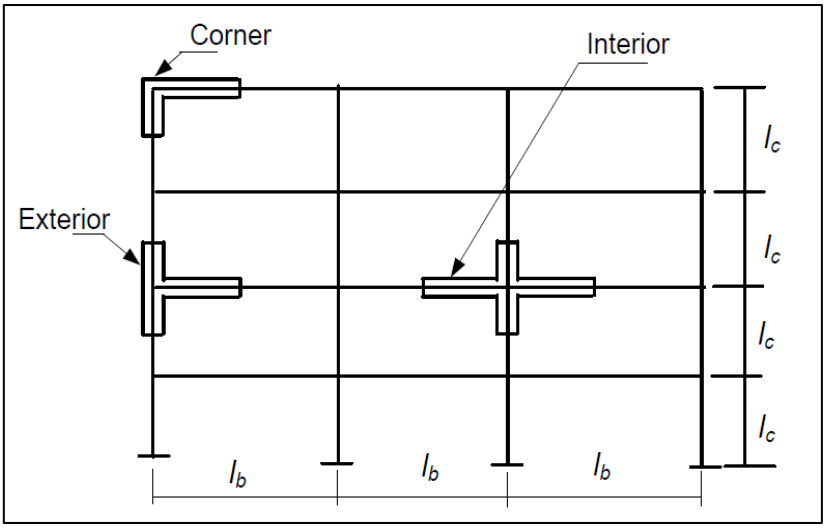

Figure 1.2 Typical frame with beam column joint

(Source: Uma and Prasad, 2015)

1.3 CARBON FIBER REINFORCED POLYMER (CFRP)

Carbon Fiber Reinforced Polymer (CFRP) is a material made up of two components: a base or carrier substance, also known as the matrix, and a second reinforcing component, the carbon fiber, which is embedded in the matrix. Typically, a synthetic resin is used as the matrix material. The mechanical properties of the cured composite vary depending on the type of carbon fibers used, the matrix, and the manufacturing process. The type of additives used in the binding matrix can have an impact on the final properties of the CFRP product. Silica is the most commonly used additive, but other additives such as rubber and carbon nanotubes can also be used. Figure 1.3 depicts a roll of CFRP plate. The effect of FRP wrapping improves the retrofitted specimens' energy absorption capacity, ductility, and stiffness (Ganesan et al., 2007). CFRP is a more expensive material than its construction industry counterparts, Glass Fiber-Reinforced Polymer (GFRP) and Aramid Fiber-Reinforced Polymer (AFRP). Though

CFRP is generally regarded as having superior properties, cost remains an issue, as do long-term durability concerns.

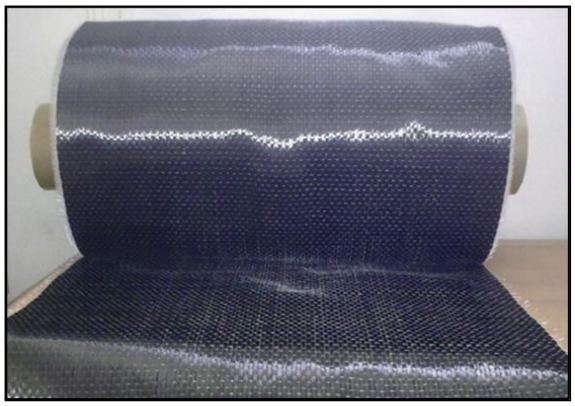

Figure 1.3 CFRP plate roll

(Source: Roberto et al., 2014)

CFRP has emerged as a significant material in structural engineering applications. It has also proven to be cost-effective in a variety of field applications, including the reinforcement of concrete, masonry, steel, cast iron, and timber structures (Hashemi et al., 2022). There is no need to drill into the structure to secure bolts or other mechanical anchors for attaching CFRP sheets, so there is no risk of causing damage to the existing reinforcement. CFRP properties and performance can be tailored to the application by varying the strength, length, directionality, and amount of reinforcing fiber, as well as the polymer matrix used (Sheela and Geetha, 2012). CFRPs can be expensive to manufacture, but they are widely used in applications requiring a high strength-to-weight ratio and stiffness, such as aerospace, ship superstructures, automotive, civil engineering, sports equipment, and an increasing number of consumer and technical applications.

1.4 SIGNIFICANCE OF THE STUDY

Beam column joints have a significant impact on a structure's response. An analytical study of the behavior of this joint provides a thorough understanding of its structural behavior as well as its significance in a structure subjected to gravity and earthquake loads. Retrofitting of structures has become a major issue worldwide due to increase in applied loads, human error in initial construction, legal requirements to comply with updated versions of codes, or the loss of strength over time. Beam-column joint regions are one of the most critical parts of reinforced concrete (RC) load-carrying structural systems, particularly during seismic events when shear demands are significantly

higher due to lateral inertia forces, resulting in brittle failures (Shang et al., 2016). As a result, the joint behavior has a direct impact on the overall structure's capacity. To avoid such failures, several strengthening techniques for weak beam column joints were developed. Figure 1.4 depicts the attachment of CFRP sheets to the beam column joint. The confinement of the CFRP wrap improves the compressive strength of the concrete in this application. Most of the research has concentrated on the behavior of reinforced concrete beam column joints or steel beam-column joints. Furthermore, very few analytical studies on the behavior of any structural form of retrofitted beam column joint have been conducted. As a result, in this study, the behavior of beam column joint retrofitted with carbon fiber reinforced polymer is numerically investigated. Nonlinear analysis is performed using the Abaqus software. Current provisions in Indian codes of practice such as IS 1893:2002, IS 13920:1993, and IS 456:2000 is inadequate in terms of (i) beam/column flexural ratio, (ii) minimum column width, (iii) estimation of shear demand, (iv) assessment of shear strength, design and detailing of shear reinforcement. Analytical research on the behavior of a retrofitted beam column joint aids in a thorough understanding of its structural performance. Numerical analysis provides a better understanding of the potential use of CFRP as a retrofitting material in critical areas such as beam column joints.

Figure 1.4 Fixing CFRP sheets to beam-column joint

(Source: Rodríguez et al., 2021)

1.5 GAPS IDENTIFIED

The research gaps identified form the literature survey were as follows: -

1. Studies on the optimum number of layers of CFRP required for retrofitting were not available.

2. Effect of orientation of CFRP sheet on retrofitted beam column joint were not studied.
3. Studies on the different anchorage methods used for placing CFRP sheets on a beam column joint were very less.
4. Literature sources on numerical analysis of CFRP retrofitted beam column joint were very less.

1.6 OBJECTIVES OF THE STUDY

The objectives of the study are as shown below:

1. To study the effect of number of layers of CFRP sheet on the behaviour of retrofitted beam column joint.
2. To study the effect of orientation of CFRP sheet on the behaviour of retrofitted beam column joint.
3. To determine the first crack load of all retrofitted models.
4. To analyse the retrofitted beam column joint models in terms of crack propagation, ductility, stiffness degradation and energy dissipation capacity.

1.7 SCOPE OF THE STUDY

The study was restricted to non-linear static analysis of exterior beam-column joint retrofitted using carbon fiber reinforced polymer. Design codes ACI 318M-02 and ACI 352R-02 were used for beam-column joint design. The analytical study was conducted using ABAQUS software.

1.8 ORGANIZATION OF THE REPORT

The thesis work is divided into nine chapters. Chapter one gives a brief description about significance of beam column joint, retrofitting using carbon fiber reinforced polymer, and significance, gaps, objectives and scope of the present work. Chapter two deals with the literature survey and it is broadly classified into exterior beam column joint and interior beam column joint. Chapter three discusses about research methodology adopted in this study. It mentions about the steps followed in this study which are namely design, modelling, analysis, parametric study and comparative study

conducted for exterior beam column joint. Chapter four gives the results of validation of Abaqus software. Chapter five shows the steps involved in the design of exterior beam column joint based on codes ACI 318M-02 and ACI 352R-02. Chapter six explains in detail about the modelling of concrete, steel and CFRP. It also mentions about the loading, boundary conditions and meshing adopted for various models. Chapter seven reports about the results obtained after analysis of various models. Chapter eight summarizes and concludes the work.

CHAPTER 2

LITERATURE REVIEW

2.1 GENERAL

This chapter provides a critical analysis of prior studies conducted across the globe on the subject of retrofitting of beam column joints using CFRP sheets. Literatures pertaining to the idea of retrofitting a beam column joint were also investigated. Additionally, literatures regarding the performance of retrofitted interior and exterior beam column joints are covered separately in this chapter.

2.2 EXTERIOR BEAM COLUMN JOINT

Kianosh et al. (2022) conducted analysis on three externally strengthened specimens to avoid potential CFRP debonding. All specimens underwent surface preparation and grooving prior to CFRP installation. Using a newly created analytical technique, the flexural capacity of both the non-strengthened and strengthened joints were calculated. When compared to the control, the externally strengthened joints demonstrated improvements in lateral load-bearing capacity, energy dissipation, and secant stiffness respectively. Furthermore, it was discovered that, despite the effectiveness of the shear retrofit design suggested for 3D outside connections, those strengthened with a combination of spike anchors and CFRP sheets performed better than those strengthened purely with CFRP sheets.

Rodríguez et al. (2021) created an analytical model to predict the shear capacity of Carbon Fiber Reinforced Polymer reinforced structures (CFRP). The axial load was applied at the surface's column top and held constant throughout the test. Cyclic loading was applied at free end of the beam. The results showed that strengthening the beam column joint with CFRP increased structural stiffness, strength, and energy dissipation capacity. When comparing the retrofitted with CFRP specimen to the normal specimen without CFRP wrapping, it was discovered that the stress in the specimen was lower in the specimen retrofitted with CFRP.

Obaidat et al. (2019) conducted an experimental investigation on the behavior of repaired RC beam-column connections under cyclic loading with a retrofitting strategy employing carbon fiber-reinforced plastics (CFRP) plates. Under cyclic loading, the specimen was tested to failure. All repaired joints have improved strength,

approaching the beam-column joint's existing shear strength. The repaired joints had significantly higher strength-capacity than the reference joints. The use of CFRP-plates significantly increased the load-carrying capacity of joints, while the mode of failure changed from diagonal cracks to debonding of CFRP-plates in retrofitted joints.

Sharma and Bansal (2019) conducted an experimental study to assess the efficiency of ultrahigh-performance hybrid fiber reinforced concrete (UHP-HFRC) retrofitting, as well as the effect of initial damage on the performance of (UHP-HFRC) retrofitted exterior beam column joint. The test results showed that retrofitting with UHP-HFRC improves the load carrying capacity, energy dissipation, and ductility of the retrofitted beam-column joint over the control specimen. When compared to the control specimen, the load hysteresis behavior of the retrofitted beam column joint improved significantly. The lateral deformation capacity of retrofitted specimens improved by 14.28 % over the control specimen, and this improvement was also dependent on the initial damage level of the retrofitted specimen.

Wang et al. (2019) investigated the use of carbon fiber reinforced polymer to strengthen seismically deficient RC beam-column joints. As strengthening options, both externally bonded CFRP sheets and near-surface mounted (NSM) CFRP strips were investigated. The test results demonstrated that adding CFRP reinforcement significantly improved the seismic performance of a seismically deficient beam-column joint. The use of NSM CFRP strips in beams and joints was discovered to effectively relocate the plastic hinge away from the joint region, resulting in a ductile failure mode.

AbuTahnat et al. (2018) investigated the ductility behavior of R.C exterior joints strengthened by FRP using numerical analysis using commercial finite element-based software. The developed F.E. model produced realistic and accurate results while capturing the joint's nonlinear complex behavior. The results showed that wrapping a beam column joint with CFRP converted brittle failure to ductile failure. Stirrup’s continuity within the joint helped to increase the capacity and ductility in shear failure models.

Esmaeeli et al. (2015) investigated the effectiveness of a repair strategy for damaged RC beam-column joints that combines strain hardening cementitious composite (SHCC) and laminates of carbon fiber reinforced polymers (CFRP laminates). The effectiveness of these retrofitting configurations was evaluated and compared

experimentally by measuring the hysteretic response, dissipated energy, degradation of secant stiffness, displacement ductility, and failure modes of each repaired specimen. The results showed that the retrofitting strategies used can restore and improve the performance of beam-column joints, as well as significantly improve the seismic performance of these specimens.

Mahmoud et al. (2015) investigated the structural performance of reinforced concrete (RC) exterior beam–column joints rehabilitated with carbon-fiber-reinforced polymer (CFRP). To repair the defective beam–column joints, three different strengthening schemes were used, including externally bonded CFRP strips and sheets as well as near surface mounted (NSM) CFRP strips. The ultimate capacity, mode of failure, initial stiffness, ductility, and ultimate strain developed in the reinforcing steel and CFRP were all considered and compared for each group of control and CFRP strengthened specimens. The results of the tests revealed that the proposed CFRP strengthening configurations were the best option for strengthening.

Hadi and Tran (2014) investigated a new method for retrofitting reinforced concrete (RC) exterior beam column T joints with segmental circular concrete covers and Carbon Fiber Reinforced Polymer (CFRP). The results of the tests revealed that the performances of both the strengthened and repaired connections were significantly improved. To resist shear load, the glued concrete covers worked well with the existing concrete. Furthermore, the wrap on the modified circular sections contributed to the increased effectiveness of CFRP by increasing the confinement effect on the concrete and reducing the possibility of CFRP debonding at the joints.

Ha et al. (2013) investigated the seismic strength and performance of reinforced concrete exterior beam–column joints using embedded carbon fiber-reinforced polymer (CFRP) bars combined with CFRP sheets in an experimental study. Under cyclic load reversals, a series of reinforced concrete exterior beam–column joint specimens were tested and investigated. The results showed that using embedded CFRP hexagonal bars in conjunction with externally bonded CFRP sheets not only increased the ultimate load-carrying capacity, displacement ductility, and energy dissipation capacity of non-seismic designed reinforced concrete beam–column joints, but also reduced flexural cracks and concrete damage near the joint.

Dalalbashia et al. (2012) conducted numerical analysis of three RC joints that have been retrofitted with FRP to determine if FRP composites are effective at enhancing the performance of the beam to column joints by relocating the plastic hinges away from the joint core. A novel retrofitting method at beam-column joints was included in the evaluation of various FRP application configurations, and the effectiveness of each composite architecture in moving the plastic hinge was explored. According to the findings, the newly suggested arrangement was not only capable of moving plastic hinges and enhancing the joints' capacity to bear weight, but it was also capable of avoiding the common interface failure.

Le-Trung et al. (2010) investigated the shear capacity of non-seismic joints strengthened with Carbon Fiber Reinforced Plastic (CFRP) materials in an experimental study. Retrofitted specimens with various configurations of CFRP sheets were developed and tested to determine an effective method of improving the seismic performance of the joints in terms of lateral strength and ductility. According to the test results, appropriately adding CFRP composites to the non-seismic specimen significantly improved the lateral strength and ductility of the test specimens. The X-shaped wrapping configuration resulted in better ductility and strength performance. The L-shaped sheets were ineffective at increasing both strength and durability.

2.3 INTERIOR BEAM COLUMN JOINT

Ong et al. (2022) reviewed the various confinement approaches that have been suggested to upgrade faulty beam-column joints. Critical analysis was performed on the testing procedure, influential parameters, effectiveness, and dependability of the confinement approaches. The important seismic features of beam-column joint are described. Finally, suggestions were given for future research and practice adoption.

Al-Rousan and Alkhawaldeh (2021) investigated the efficiency of external FRP composites in improving structural performance and controlling the mode of failure of the reinforced concrete (RC) beam-column joint with different bond strength degradation percentages using nonlinear finite element analysis. The analysis results revealed that the FRP strengthening technique with bond strength degradation percentages less than 30% improved cyclic performance and performed well in eliminating any surface debonding or buckling in the FRP composite due to the proper lateral support provided for the FRP composite.

Al-Rousan et al. (2021) investigated the efficiency of incorporating CFRP composites for improving the response of interior Beam-Column (B-C) connections when subjected to axial and lateral cyclic loads. The configuration, orientation, length, and number of layers of CFRP sheets were among the parameters considered. According to the nonlinear FEA results, the used strengthening schemes of CFRP composites can significantly improve the B-C connection performance, resulting in higher lateral load and drift capacities as well as energy dissipation. As the bonding area increased, so did the effectiveness of the used CFRP composite. The orientation angle of the CFRP sheets had a significant impact on energy dissipation but a minor impact on ultimate lateral load and corresponding drift.

Elsanadedy et al. (2021) investigated the efficiency of using an innovative hybrid strengthening technique composed of near-surface mounted (NSM) steel rebars and fiber reinforced polymer (FRP) sheets to prevent progressive collapse in precast reinforced concrete (RC) beam-column joints through experimental and numerical analysis. The innovative CFRP/NSM technique was used to retrofit precast RC beam-column joints, which significantly improved the load–displacement characteristics under column-loss scenarios. The strengthening technique was found to be effective in reducing the risk of progressive collapse of precast RC frames, particularly during the flexural action phase.

Akhlaghi and Mostofinejad (2020) investigated the effect of using carbon-fiber reinforced polymer (CFRP) composites to improve the lateral strength capacity of interior reinforced concrete (RC) beam-column connections. Four different anchorage systems have been evaluated to provide continuity for composites across the joint. The experimental results demonstrated that the 180-degree anchor fan outperformed all other tested anchorage systems, resulting in a complete plastic hinge relocation along the beam from the column face. The EBROG technique eliminated both surface debonding and compressive buckling failure of composite sheets bonded on the top and bottom sides of the beam.

Ilia and Mostofinejad (2019) conducted an experimental study to assess the efficacy of rehabilitation schemes for retrofitting deficient RC beam-column connections with fiber reinforced polymers (FRPs). Specimens were strengthened with CFRP sheets using the externally bonded reinforcement on grooves (EBROG) method. The test

results demonstrated that the adopted strengthening schemes successfully prevented brittle failure of the specimens. It was also observed that the EBROG technique, in conjunction with the CFRP fans at the interface of the beam-column joints, effectively eliminated any debonding or slipping of the longitudinal CFRPs, and that CFRP retrofitting schemes were capable of effectively improving the seismic performance of the deficient beam-column joints in terms of load-carrying capacity, ductility, and energy dissipation.

Jiajia et al. (2019) experimentally analyzed seven double shear specimens by conducting double shear tests on the contact between sprayed FRP and concrete substrate. The distribution of strain and stress, load and deformation, shear strength and deformation, and failure mode were investigated. The impact of three key parameters, including the fiber volume ratio, FRP thickness, and bonding length, was also examined in the article. The findings demonstrate that while fiber volume ratio has no effect on the bonding mechanical properties, the thickness of sprayed FRP and bonding length do. Only up to a certain length can the bonding contact contribute in sustaining shear load before moving from the loading end to the other end as debonding develops.

Mostofinejad and Hajraouliha (2019) studied the shear strength of non-seismic 3D joints that lack adequate transverse reinforcement in their joint panel but are reinforced with carbon fiber reinforced polymer (CFRP) sheets. In the joints, the externally bonded reinforcement on groove (EBROG) technique was used to delay the debonding of CFRP sheets from the concrete substrate. The specimens were strengthened with X-shaped patterns. According to the findings, the proposed strengthening pattern prevented joint shear failure. Furthermore, the proposed EBROG technique outperformed the externally bonded reinforcement (EBR) techniques, as evidenced by higher maximum load-carrying capacity and ductility values recorded by the joint, while CFRP debonding from the concrete substrate was also delayed.

Yalçin et al. (2019) carried out an experimental study to predict the lateral load capacities of shear-critical joint subassemblies with and without carbon fiber-reinforced polymer (CFRP) wrapping. For each incremental lateral load level, several failure mechanisms such as shear failure in the joint panel, crushing of concrete in the beam, yielding of the beam reinforcement, or rupture of CFRP wrapping were determined, and the most critical ultimate lateral load capacity was obtained. The developed model

revealed that concrete compressive strength, the use of smooth steel bars, joint transverse reinforcement, and in-plane geometry could all play significant roles in determining joint shear capacity.

Mahmoud et al. (2014) conducted an experimental study to investigate the structural performance of reinforced concrete (RC) interior beam–column joints that had been rehabilitated with carbon-fiber-reinforced polymer (CFRP). According to the test results, the proposed CFRP strengthening configurations were the best choice for strengthening the first two defects in terms of the studied failure criteria. It was also discovered that strengthening the joint with the NSM strip technique allowed the specimen to outperform the structural performance of the control specimen, whereas strengthening the joints with externally bonded CFRP strips and sheets failed to restore the strengthened joints capacity.

Mostofinejad et al. (2014) conducted an experimental study on reinforced concrete (RC) beam specimens flexurally strengthened by fiber-reinforced polymer (FRP) sheets using conventional externally bonded reinforcement (EBR) and grooving method (GM) techniques in the form of externally bonded reinforcement on grooves (EBROG) and externally bonded reinforcement in grooves (EBRIG). By postponing the debonding phenomenon, both EBROG and EBRIG techniques significantly improved the load-carrying behavior of beams strengthened with two and three layers of FRP sheets. When compared to conventional methods, GM via EBROG and EBRIG appears to control the debonding of FRP sheets from concrete substrates more effectively.

Unal et al. (2013) studied the seismic performance of a half-scale, three-story, three-bay RC frame's interior beam-to-column connection regions. The RC moment resistant frame building was developed in accordance with code standards, and pseudo-dynamic testing was used to simulate earthquake excitations of varying intensities applied sequentially to the frame. At the conclusion of the testing, it was discovered that the strength of the members had been exceeded by the strong seismic stresses, and a collapse mechanism had developed. Investigations were also conducted into the relationships between the responses of the beam and joints, the impact of connection quality on the seismic response of the frame, and the impact of various soil types.

Seyed et al. (2010) studied the use of web-bonded FRP (fiber reinforced plastic) in a broken joint whose structural strength was severely compromised. The outcomes

demonstrated the method's efficiency and ability to restore or even increase the system's strength. In addition, an analytical model was developed that simplifies the analysis and construction of this strengthening scheme using the fundamental concepts of equilibrium and compatibility. A variety of design graphs were shown based on the model for choosing the type and quantity of FRP needed to upgrade an existing joint to a specific moment capacity and curvature ductility.

Lee et al. (2010) used both experimental and numerical methods to predict the column shear of joints reinforced with carbon fiber reinforced polymer (CFRP). The specimens were intended to represent a pre-seismic code design construction with no transverse reinforcement. The experimental results showed that strengthening the beam–column joints with CFRP increased structural stiffness, strength, and energy dissipation capacity. The rehabilitation strategy was effective in increasing joint ductility and converting the failure mode to beam or delaying the shear failure mode. It has been discovered that mechanical anchorages can prevent CFRP debonding.

2.4 SUMMARY

The effectiveness of retrofitted beam-column joints and the advantages of employing CFRP sheets on the interior and exterior beam column joints have been the subject of research efforts. The literature review revealed that the performance of CFRP was superior. The load-carrying capability was greatly boosted by retrofitting using CFRP sheets. The use of CFRP composite as an external strengthening approach led to improvements in ductility, energy dissipation, and stabilized stiffness deterioration. Diagonal cracks were replaced by debonding of CFRP plates in joints that had been modified as the failure mode. It was noted that there had been no prior research on parameters like number of layers of CFRP sheets with different fiber orientations and the most suitable orientation for a given area of CFRP sheets.

CHAPTER 3

RESEARCH METHODOLOGY

3.1 GENERAL

Exterior beam column joint structural model was considered for analysis. Numerical investigation of structures offers an attractive technique of research due to low cost, quick results and ability to study several variables in depth. Therefore, a three-dimensional non-linear finite element joint model was built using commercial software Abaqus. For conducting the analysis, the first step was the validation of Abaqus software based on data from experimental analysis conducted by Mahmoud et al. (2014). For the fulfillment of the defined objectives, the steps followed were design of joint using ACI 352R-02 and ACI 318-2011, structural modelling, nonlinear static analysis, parametric study, development of force-displacement curve and comparative study. The methodology of the project is outlined as flow chart in the Figure 3.1 shown below.

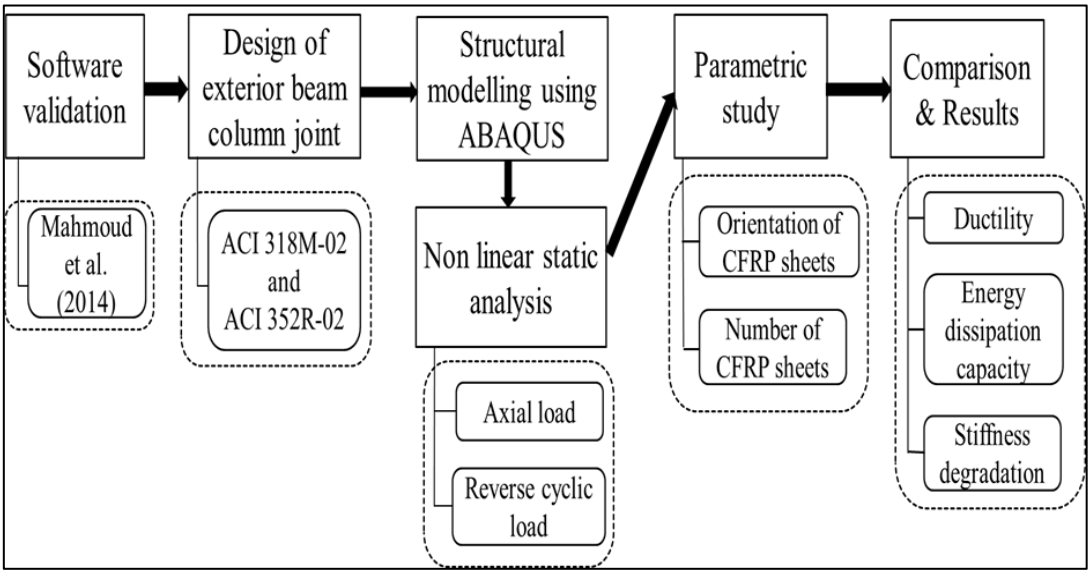

Figure 3.1 Flowchart of project methodology

3.2 DESIGN OF EXTERIOR BEAM-COLUMN JOINT

ACI 352R-02 and ACI 318M-02 were used to design the exterior beam-column joint. These codal recommendations apply only to structures made of normal weight concrete with a compressive strength of not more than 100MPa. Structural connections are classified into two types based on the loading conditions and the anticipated deformation of the connected frame members when resisting lateral loads. Type 1 connections are made up of members that do not experience significant inelastic

deformation, whereas Type 2 connections require frame members to dissipate energy and are designed to have sustained strength even when deformation reversals into the inelastic range occur.

3.3 GEOMETRIC MODELLING

A finite element model was created with the Abaqus software and used to obtain analysis results. The numerical analysis was carried out with the help of the ABAQUS software. Abaqus is a non-linear three-dimensional finite element software that is widely used in the modelling and analysis of a wide range of engineering problems. Because of its extensive material modelling capabilities, this software is extremely popular. Abaqus is divided into modules, each of which defines a different aspect of modelling. In Abaqus, the analysis process is divided into three stages. The first step is modelling, which includes creating parts, defining materials, assembling parts, defining interactions, boundary conditions, and meshing. The analysis stage follows, where the loading condition and type of analysis are defined. The last stage is the visualization, where we can see the graphical display of the finite element models and results. The results can be viewed graphically as deformed shape, contours or symbols. Based on the output requests, the X-Y data can be obtained at this stage.

3.4 NON-LINEAR STATIC ANALYSIS

The exterior beam-column joint was subjected to nonlinear static analysis. A nonlinear analysis is an analysis where a nonlinear relation holds between applied forces and displacements. Nonlinear effects can originate from geometrical nonlinearity's, material, and contact. These effects result in a stiffness matrix which is not constant during the load application. The design procedure for non-linear static analysis was as follows: -

1. A constant axial load to be applied on top of the column which corresponds to the gravity load induced by the upper floors.

2. A reversed cyclic load was to be applied at tip of beam to directly correlate the measured displacements of the joint to the inter-story drift of an entire frame. The load application was quasi-static with displacement control. It was intended to ensure that the applied reversed cyclic load was increased gradually in steps, neither too large nor too small. This was followed by an incremental load applied as displacement control.

4. Maximum principal stress, total deformation and force reaction in the direction of deformation were to be obtained.

5. From the results, force displacement graph was plotted to give a clear idea on the performance of both the joints. It also helps to carry out a comparative study between the performance of normal beam column joint and retrofitted beam column joint.

3.5 PARAMETRIC STUDY

The behavior of a CFRP retrofitted beam column joint depends on many parameters like orientation, number of layers, length, and anchorage methods adopted for attaching CFRP. Parametric study was conducted to investigate the behavior of retrofitted exterior beam column joint strengthened by CFRP. Two main parameters were investigated in this study. They were the orientation of CFRP sheet and number of layers of CFRP sheet.

3.6 COMPARATIVE STUDY

The analysis results were displayed in the visualization module. This module obtains the output data requested in the step module. The deformation of the joint in the direction of the applied load verses time was obtained as the X-Y plot. Load was defined as a linear function of time in the obtained plot. Thus, the load verses displacement graph can be created by combining the data of load versus time and displacement versus time from the X-Y data. Load deformation graphs were created for retrofitted joint models. The ductility, energy dissipation capacity, and stiffness degradation of joints can be calculated by analyzing the load displacement graph. The outcomes of analysis of the retrofitted joints were compared with that of normal joint to understand the improvement in structural performance of CFRP retrofitted beam column joint.

3.7 SUMMARY

The parametric study provided a better understanding of the effect of orientation of CFRP sheet and number of layers of CFRP sheet on the performance of a retrofitted beam column joint. Also, a comparative study based on ductility, energy dissipation and stiffness degradation of retrofitted joints and normal joint provided in-depth analysis of performance of joint. To compare the performance of both normal beam column joint and retrofitted joint, the force-displacement curve developed from the results can be used as an important tool.

CHAPTER 4

VALIDATION

4.1 GENERAL

The Abaqus software was validated using the results published by Mahmoud et al. (2014). He conducted the experiment to investigate the behavior of reinforced concrete (RC) exterior beam–column joints that had been rehabilitated with Carbon-Fiber-Reinforced Polymer (CFRP).

4.2 MODELLING AND ANALYSIS

The experiment was carried out on ten half-scale specimens divided into three groups to cover three possible defects, namely the absence of transverse reinforcement within the joint core, insufficient bond length for the beam main reinforcement, and an inadequate spliced implanted column. Ultimate capacity, mode of failure, initial stiffness, ductility, and ultimate strain in reinforcing steel and CFRP were among the failure criteria investigated. The experimentally analyzed model was simulated in Abaqus software. The model was created as same as the experimental setup and was made of M20 grade concrete. The overall length of the beam was chosen as 800 mm and cross-sectional dimensions as 250 x 350 mm. This beam was connected to a column at its mid-height point. The cross-section of the column was 350 x 250 mm. The total height of the columns was 2000 mm divided into two equal parts, lower part and upper part. The main steel reinforcement of the beam was three bars of 16 mm diameter, while the secondary steel reinforcement was two bars of 12 mm diameter. On the other hand, the column was reinforced with four bars of 16 mm diameter at each corner of the column cross-section. The stirrups for both beam and column were mild steel bars of 8 mm diameter and spaced every 100 mm and 150 mm for the beam and the column, respectively. Material properties of joint is mentioned in table 4.1.

Table 4.1 Material properties of beam-column joint from experimental data

Input Parameter	**Steel**	**Concrete**
Density	7800 kg/m^3	2400 kg/m^3
Young’s modulus	200000 MPa	25000 MPa
Poisson’s ratio	0.30	0.12
Yield strength	250 MPa	3.50 MPa

Figure 4.1 depicts the experimental test setup. The bottom end of the column was fixed, while the other end was subjected to a point load to hold the column in place, and the beam was loaded to failure. Steel caps were used at both ends of the column to distribute the column compression load at the upper end and to support the lower end of the column at the testing frame. In addition, a threaded rod was wrapped around the upper steel cap and fastened to the testing frame's column to prevent the specimen from tilting during testing.

Figure 4.1 Test setup

(Source: Mahmoud et al., 2014)

A compression load equals to 200 KN, simulating the load in a real structure, was first applied to the column before the beam was loaded. During the loading phase, the column load was kept constant and the beam was loaded to failure in stages. The joint model developed in Abaqus is shown in figure 4.2. Meshed model with mesh size of 40 and 25 is shown in figure 4.3 and figure 4.4. Deformed model of joint after loading stage is shown in figure 4.5.

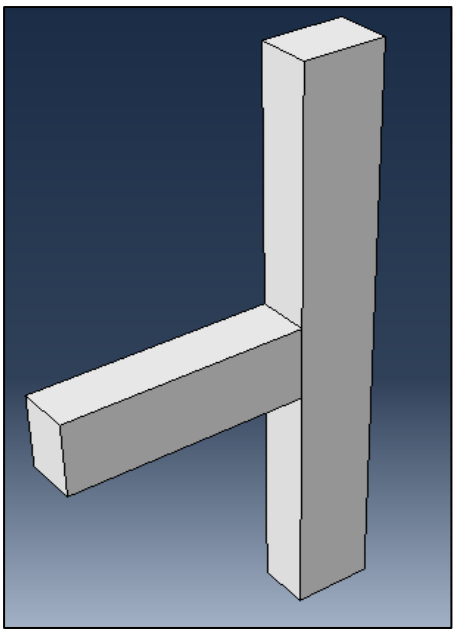

Figure 4.2 Beam column joint model

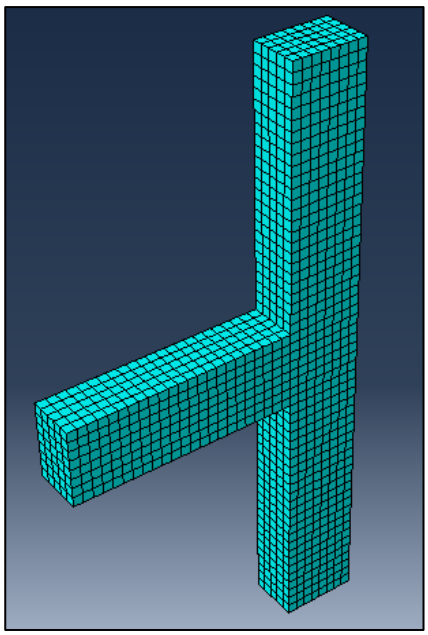

Figure 4.3 Meshed model
(Mesh size – 40)

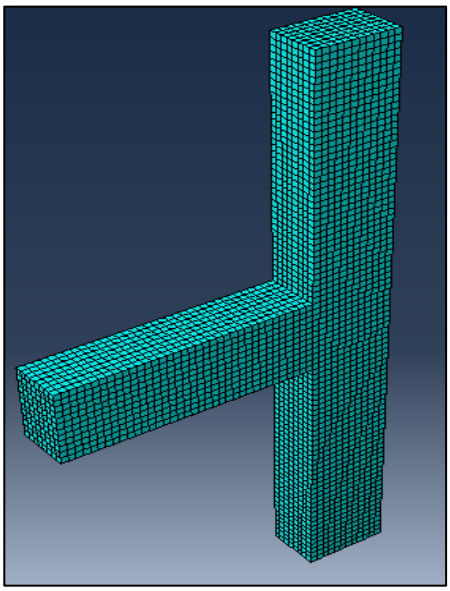

Figure 4.4 Meshed model
(Mesh size- 25)

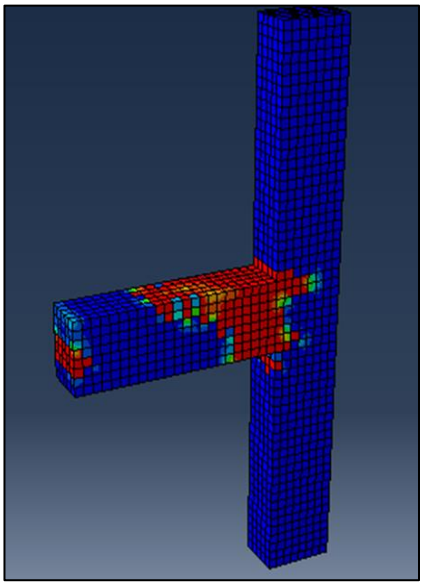

Figure 4.5 Deformed model

Figure 4.6 shows the graph comparing the published experimental results and finite element results obtained. In order to analyze mesh size sensitivity of the numerical model in this study, the finite element analysis results of the exterior joint specimen with 40 mm and 25 mm element mesh sizes were considered. From the graphs it could be seen that the finite element results were in close agreement with the experimental results in case of both mesh sizes of 25 mm and 40 mm.

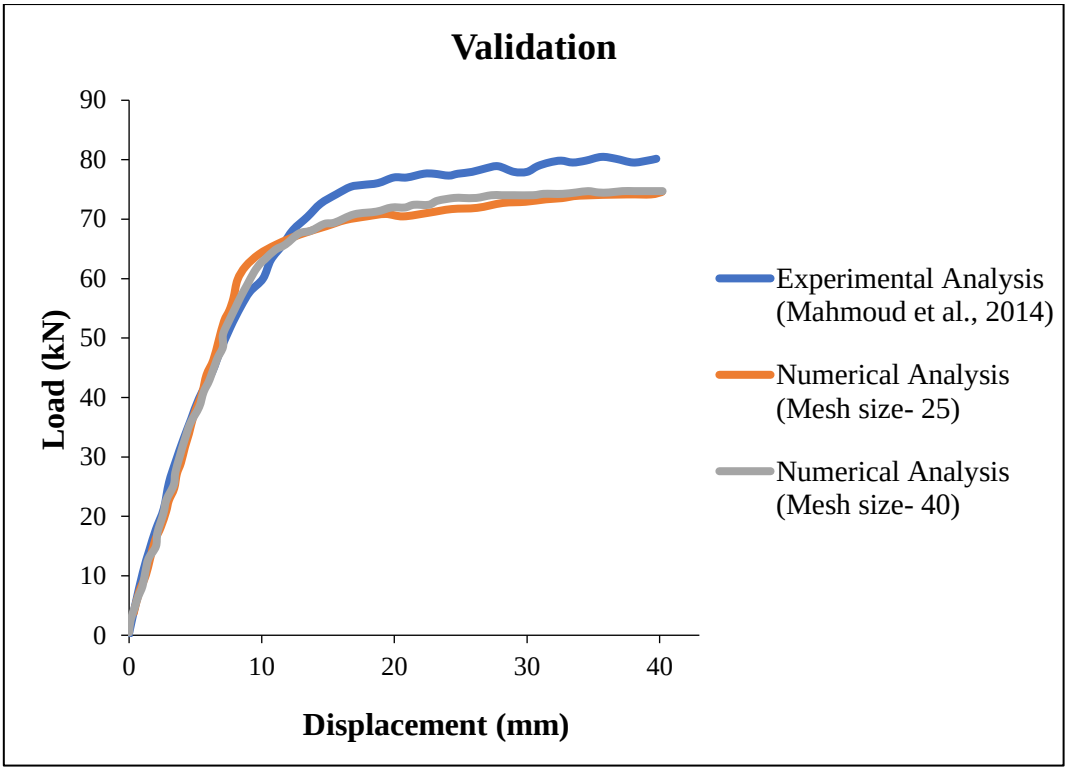

Figure 4.6 Load-displacement curve of experimental and numerical analysis

Table 4.2 Comparison of ultimate load and displacement of joint

Parameters	**From experimental analysis**	**From numerical analysis**			
		Mesh size - 40		**Mesh size - 25**	
Ultimate Load (kN)	79.80	76.80	3.75 %	77.20	3.26 %
Displacement (mm)	40.20	38.80	3.48 %	39.50	1.74 %

The ultimate load value and displacement value from the numerical analysis and from the experimental analysis were tabulated below in Table 4.2. A variation of 7.01% and 3.48% were observed in ultimate load and displacement values respectively for mesh size 40. For mesh 25, variation in ultimate load and displacement is 5.26% and 1.74%. Since the difference was less than 10% the software and model can be used for analysis. The parity curve for displacement was shown in figure 4.8 and the variations between load values for experimental and numerical analysis for mesh size 40 mm and mesh size 25mm was found to be 4° and 2.5° respectively. As shown in figure 4.9 for parity curve for load, the variation between experimental analysis and finite element analysis for mesh size 40mm and 25 mm were found to be 3.5° and 3° respectively.

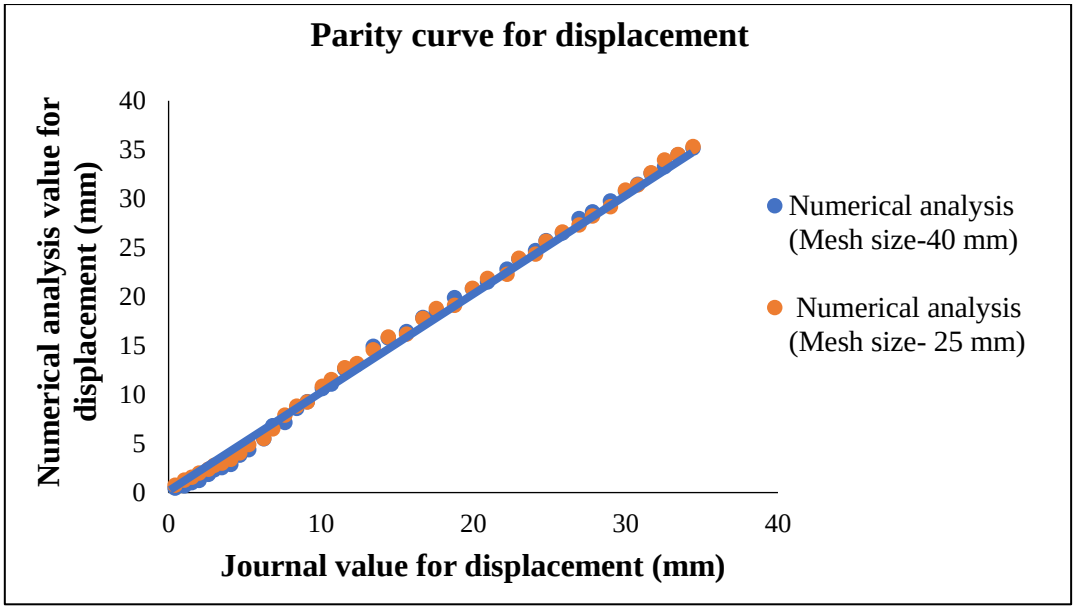

Figure 4.7 Parity curve for displacement

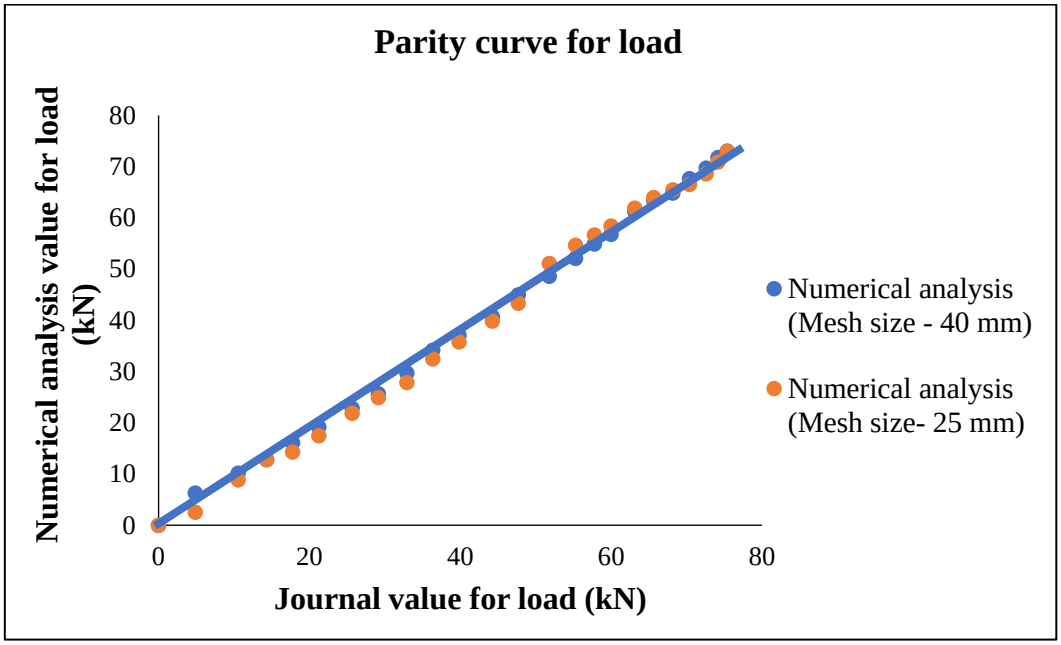

Figure 4.8 Parity curve for load

4.3 SUMMARY

Although the effects of mesh size and strain localization in the numerical model were within the margins of error expected for most numerical simulations based on plasticity models, slight differences in peak lateral loads and displacements were observed. The slight differences may be due to the variations in the unknown assumptions made in defining properties of materials and in defining the interaction between reinforcement and concrete.

CHAPTER 5

DESIGN OF EXTERIOR BEAM OLUMN JOINT

5.1 GENERAL

Exterior beam-column joint is designed using ACI 352R-02 and ACI 318M-02. Only structures made of normal weight concrete with a compressive strength of less than 100 MPa are covered by these codal recommendations. The Type 2 connection was selected for joint design in this investigation.

5.2 DESIGN STEPS

The following are the steps involved in designing the beam column joint:

Step 1: Determine the material properties and the beam-column joint dimension

The material properties of the beam-column joint that is to be designed for analysis are as follows:

Table 5.1 Material properties of the beam-column joint

Parameter	Steel	Concrete
Density (kg/m3)	7800	2400
Young's modulus (MPa)	200000	25000
Poisson's ratio	0.30	0.15

Dimensions of exterior beam column joint are as follows:

Column - cross section of 300 mm x 200 mm and height of 2300 mm

Beam - 200 mm x 300 mm cross section and length of 900 mm

Step 2: Calculate the amount of reinforcement

Section 10.9.1 of ACI 318-2011 specifies that the area of longitudinal reinforcement for non-composite compression members should not be less than 0.01 times the gross section of the column and should not be greater than 0.08 times the gross section of the column. Section 10.5.1 of ACI 318-2011 requires beam reinforcement as shown in equation Eq. 5.1. In Eq. 5.2, A_{smin} represents the minimum area of reinforcement, f_c' represents the compressive strength of concrete, b_w represents the web width of the beam, d represents the depth of the beam, f_y represents the yield strength of steel, and

A_s represents the area of steel reinforcement. Section 7.10.5.1 of ACI 318-2011 requires at least 8mm diameter ties for longitudinal bars of 30mm or less.

$$\text{Minimum reinforcement, } A_{smin} = (3\sqrt{f_c'}b_w\, d)/f_y \qquad \text{Eq. 5.1}$$

$$= (3*\sqrt{30}*200*300)/415$$

$$= 2375 \text{ mm}^2$$

$$\text{Area of steel reinforcement, } A_{st} \leq (200b_w d) / f_y \qquad \text{Eq. 5.2}$$

$$\leq (200*200*300)/415$$

$$\leq 28915 \text{ mm}^2$$

Step 3: Calculate the design shear force of beam-column joint

The magnitude of the shear force of the joint V_u is calculated by finding the difference in the amount of tension and compression to the horizontal shear force that works on the column as given by equation Eq. 5.3, where C_s and T_s are the beam compression and tension forces given by equations Eq. 5.4 and Eq.5.5 and V_c is the horizontal shear force on the column, α is the stress multiplier for longitudinal reinforcement and is equal to 1.25, f_y is the yield strength of steel, The equation Eq. 5.8 gives the column shear force, where M_{prb} is the beam moment, h is the column height, A_s is the sum of top and bottom beam longitudinal reinforcement (Eq. 5.7), d is the beam depth, f_c' is the concrete compressive strength, and b is the beam breadth. The shear force of the joint is to be calculated using all of the above equations and appropriate values.

$$\text{Design shear force of the joint, } V_u = (T_s + C_s) - V_c \qquad \text{Eq. 5.3}$$

Sum of top and bottom beam longitudinal reinforcement,

$$A_s = A_{s1} + A_{s2}$$

$$= 2*0.78*122+3*0.78*162$$

$$= 1005.32 \text{ mm}^2$$

$$\text{Beam compression force, } C_s = \alpha\, f_y\, A_s \qquad \text{Eq. 5.4}$$

$$= 1.25*415*603$$

$$= 312.91 \text{ kN}$$

$$\text{Beam tension, } T_s = \alpha\, f_y\, A_s \qquad \text{Eq.5.5}$$

$$= 1.25*415*224.64$$

=116.53 kN

$a = (A_s \alpha f_y) / (0.85 f_c' b)$ Eq.5.6

= (10005.32*1.25*415)/ (0.85*30*200)

= 102.26

Beam moment, $M_{prb} = 2 A_s \alpha fy (d- a/2)$ Eq. 5.7

= 2*1005.32*1.25*415*(300-51.13)

=259.58 kNm

Horizontal shear on column, $V_c = M_{prb} / h = (259.58/2.3)$ Eq. 5.8

=112.86 kN

Design shear force of the joint, $V_u = (T_s + C_s) – V_c$

= 408.64 kN

Step 4: Calculate the concrete shear capacity of joint

Current building codes in high seismic zones require the design of reinforced beam-column joints to take joint shear failure into account. This is due to the observation that joint shear failure occurs prior to beam or column flexural yielding. Eq. 5.9 is used to calculate the concrete shear capacity V_{cs}.

Concrete shear capacity, $V_{cs} = 0.2905\sqrt{f_c'}\sqrt{(1+ 0.2903 N_u/A_g)}$ Eq. 5.9

= 0.2905√30’√ (1+ 0.2903 *100000/ (200*300)

= 110.68 kN

where Nu denotes the axial force acting on the column and Ag denotes the gross column area. The concrete shear capacity of the joint must be determined. If the axial compressive stress in the column N_u/A_g is less than 0.12 f_c', then the contribution of concrete shear resistance should be ignored.

Step 5: Calculate the joint shear strength

The horizontal shear in the joint must be checked independently in each direction in connections with beams framing in from two perpendicular directions. The design shear force V_u is computed on a horizontal plane at the joint's mid-height by taking into account the shear forces on the joint's boundaries as well as the normal tension and compression forces in the members framing the joint. Eq. 5.11 is used to calculate the joint shear strength V_n. Eq. 5.10 should also be met.

$$\varphi V_n \geq V_u \qquad \text{Eq. 5.10}$$

$$Vn=0.083\gamma\sqrt{fc'}bjhc \qquad \text{Eq. 5.11}$$

$$b_j = (b_b + b_c)/2 \qquad \text{Eq.5.12}$$

Effective width of joint transverse to the direction of shear,

$$b_j = (b_c + b_b)/2$$

$$= (200+300)/2$$

$$= 250 \text{ mm}$$

Joint shear strength, $V_n = 0.083\gamma\sqrt{f_c'}b_j h_c$

$$= 0.083*20*\sqrt{30}*250*2300$$

$$= 5228.11 \text{ kN}$$

$$\varphi V_n \geq V_u$$

$$0.85* 5228.11 \geq 408.64 \text{ kN}$$

Where φ is the strength reduction factor and equals 0.85, γ is the shear strength factor reflecting joint confinement by lateral members and equals 20, bj is the effective width of joint transverse to shear (Eq. 5.12), h_c is the full depth of column, b_b is the web-width of beam, b_c is the core dimension of tied column, and m is the slope to define the effective width of joint transverse to shear. The design philosophy embodied in Eq. 5.12 is that the joint can resist the specified shear forces if the concrete within the joint is adequately confined during anticipated earthquake loading and displacement demands.

Step 6: Design shear force of joint stirrup

The amount of design shear force that must be resisted by stirrups V_s is given by the equation Eq. 5.13.

$$\text{Design shear force, } V_s = V_u - V_c \qquad \text{Eq. 5.13}$$

$$= 433.14 \text{ kN}$$

5.3 SUMMARY

The design of exterior beam column joint had been done on the basis of design codes ACI 352R-02 and ACI 318M-02. All the design steps had been followed in order and the reinforcement required for the joint along with sufficient spacing was calculated and design forces had been obtained. The design is found to be safe in all aspects.

CHAPTER 6

GEOMETRIC MODELLING AND ANALYSIS

6.1 GENERAL

Abaqus software was used to build a finite element model and generate analysis findings. It was utilized to complete the numerical study. Abaqus, a non-linear three-dimensional finite element-based software, is a popular modelling and analysis tool for a variety of engineering tasks. This programme is quite popular because of its broad material modelling features. The analytical procedure in ABAQUS is broken down into three steps. They are modelling, analysis and visualization. Modeling was the initial phase, which entails constructing pieces, specifying materials, putting parts together, specifying interactions, setting boundary conditions, and meshing.

6.2 MATERIAL MODELLING

The exterior beam column joint was developed in Abaqus and is shown in figure 6.1. The joint possesses a vertical column with a cross section of 350 mm x 250 mm intersecting a horizontal beam with a 250 mm x 350 mm cross section. The height of the column was 2040 mm and the beam extended by 1000 mm before and after the connection. The longitudinal reinforcement of the column was 4 number of 16 mm diameter rebars and the shear reinforcement was 8 mm diameter stirrups with a spacing of 160 mm as given in figure 6.2. The beam steel reinforcement was 3 number of 16 mm diameter rebars at bottom and 2 number of 12 mm diameter bars at top, and the shear reinforcement was 8 mm diameter stirrups with a spacing of 110 mm. Clear cover of 40 mm was provided for beams and column. The details of reinforcement of joint developed in Abaqus is shown in figure 6.2.

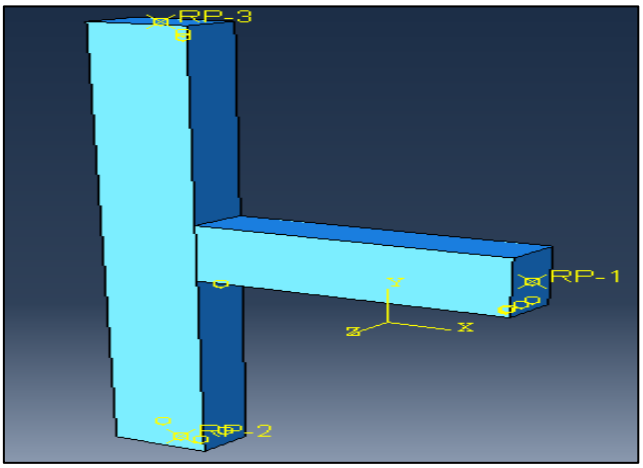

Figure 6.1 Model of the exterior beam column joint developed using Abaqus

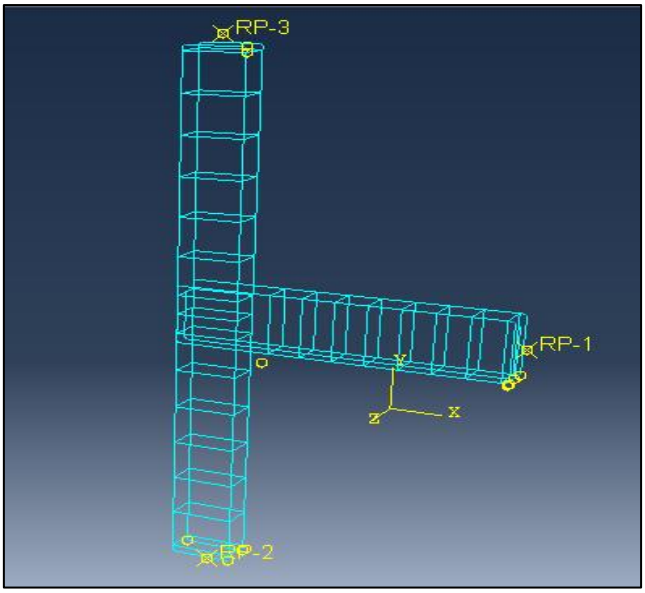

Figure 6.2 Reinforcement details of model developed in Abaqus

6.2.1 Modelling of steel

The reinforcement was modelled using isotropic behaviour. As plastic straining occurs, the yield surface changes size uniformly in all directions, causing the yield stress to increase (or decrease) in all stress directions. Table 6.1 lists the properties of steel used for joints.

Table 6.1 Properties of reinforcement for the joint

Bar Diameter (mm)	**Cross sectional area (mm^2)**	**Yield strength (MPa)**
16	200.96	400
12	113.04	400
8	50.24	240

6.2.2 Modelling of concrete

The concrete damage plasticity (CDP) model was used to simulate concrete's complex nonlinear behaviour. This model takes into account two major failure criteria: tensile cracking and compressive crushing of the concrete material. Table 6.2 shows the CDP values for M30 concrete. The CDP model captures concrete strength and stiffness degradation via tension and compression damage parameters. Table 6.3 lists the material properties of concrete for the CDP model.

Table 6.2 Concrete Damage Plasticity values for M30 concrete

(Source: AbuTahnat et al., 2018)

Parameter name	**Value**
Dilation angle (ψ)	36°
Eccentricity (e)	0.1
f_{b0} / f_{co}	1.16
K	0.667

Table 6.3 Material properties for concrete

(Source: Milad et al., 2017)

Concrete compressive behaviour		**Concrete compression damage**	
Yield stress (MPa)	Inelastic strain	Damage parameter (C)	Inelastic strain
15.3	0	0	0
19.2	0.0000482	0	0.0000482
22.5	0.0001198	0	0.0001198
25.2	0.0002147	0	0.0002147
27.3	0.000333	0	0.000333
28.8	0.0004747	0	0.0004747
29.7	0.0006397	0	0.0006397
30.0	0.00082802	0	0.00082802
29.7	0.0010396	0.01	0.0010396
28.8	0.001275	0.04	0.001275
27.3	0.001533	0.09	0.001533
25.2	0.001815	0.16	0.001815
22.5	0.00212	0.25	0.00212
19.2	0.002448	0.36	0.002448
15.3	0.0028	0.49	0.0028
10.8	0.003175	0.64	0.003175
5.70	0.0035735	0.81	0.0035735
Concrete tensile behaviour		**Concrete tension damage**	
Yield stress (MPa)	Cracking strain	Damage parameter (T)	Cracking strain
3	0	0	0
0.03	0.001167	0.99	0.001167

6.2.3 Modelling of CFRP

The R.C beam-column joint model was strengthened using unidirectional CFRP sheets. The fiber behaviour was linear elastic up to failure with rupture failure. Figure 6.3

depicts an exterior beam column joint model retrofitted with a single layer of CFRP sheet. A lamina linear elastic element was used to model CFRP. The mechanical properties for the combined CFRP sheet and adhesion are evaluated using Equations. (6.1 – 6.6) as proposed by AbuTahnat et al. (2018).

$$E_1 = E_f V_f + E_a (1-V_f) \quad \text{Eq. 6.1}$$

$$E_2 = E_f E_a / (E_a V_f + E_f (1-V_f) \quad \text{Eq. 6.2}$$

$$G_{12} = G_{13} = G_f G_a / (G_a V_f + G_f (1-V_f) \quad \text{Eq. 6.3}$$

$$G_{23} = E_2/2(1+\nu_{23}) \quad \text{Eq. 6.4}$$

$$\nu_{23} = \nu_f V_f + \nu_a(1-V_f) \quad \text{Eq. 6.5}$$

$$\sigma_{co} = V_f \sigma_u + ((1-V_f) E_a/E_f) \sigma_u \quad \text{Eq. 6.6}$$

where:

E_1: Elastic modulus in the longitudinal direction

E_2: Elastic modulus in the transverse direction

G_{12} and G_{13}: Plane shear modulus

G_{23}: Normal to the plane shear modulus

ν: Poisson's ratio

σ_{co}: Ultimate tensile strength

E_f: Elastic modulus of CFRP

V_f: Volume fraction of CFRP is provided by the manufacturer

E_a: Elastic modulus of adhesive material

G_f: Shear modulus of CFRP

G_a: Shear modulus of adhesive material

The properties of CFPR sheet used in the study is enumerated in Table 6.4. The property of adhesives used for ensuring the bond between CFRP sheet and concrete surface is mentioned in table 6.5.

Table 6.4 Properties of CFRP sheets

Fiber type	**Relative density**	**Ultimate tensile strength** (MPa)	**Ultimate strain** (%)	**Modulus of elasticity** (MPa)	**Thickness** (mm)
CFRP	1.9	3500	1.5	230000	1

Table 6.5 Properties of adhesive for installing CFRP sheets

Epoxy type	**Tensile strength** (MPa)	**Tensile modulus** (MPa)	**Ultimate elongation** (%)
Adhesive for installing CFRP	30	21400	4.8

The properties of combined CFRP sheets with matrix is elaborated in Table 6.6. Also, Table 6.7 summarizes the properties of fibres in CFRP sheets.

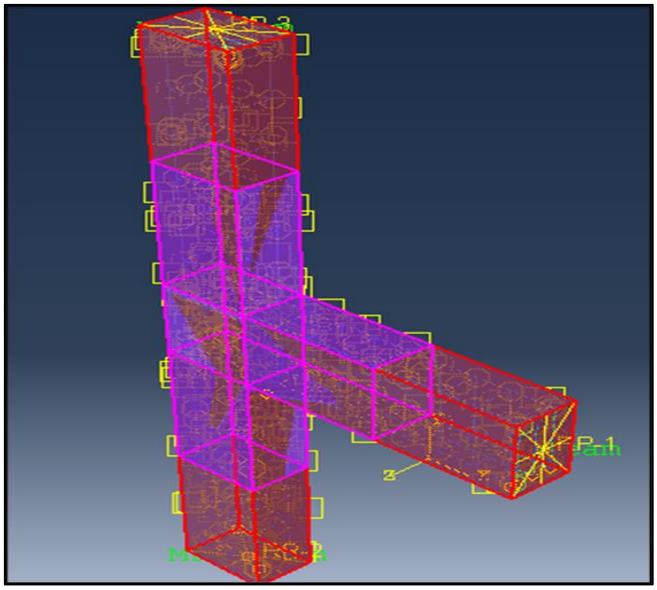

Figure 6.3 Model of exterior beam column joint retrofitted with single layer of CFRP sheet

Table 6.6 Properties for combined CFRP sheets with matrix

Type of FRP	**E_1 (MPa)**	**E_2 (MPa)**	**G_{12} (MPa)**	**G_{13} (MPa)**	**G_{23} (MPa)**
CFRP	106509	33970	12400	12400	13065

Table 6.7 Properties of fiber's in CFRP sheets

Tensile stress in fiber direction (MPa)	**Compressive stress in fiber direction** (MPa)	**Tensile stress in transverse direction** (MPa)	**Compressive stress in transverse direction** (MPa)	**Shear strength** (MPa)	**Stress limit** (MPa)
3100	0.10	3100	0.10	0.10	3100

6.3 ELEMENT PROPERTIES

For modelling concrete elements with reduced integration, 3D 8-noded hexahedral (brick) elements (C3D8R) with 3 degrees of freedom in each node translations in X, Y, and Z directions were used. To model reinforcements, 2-noded truss elements (T3D2) with three degrees of freedom in each node translations in the X, Y, and Z directions of the global coordinates system was used. To accurately simulate the reinforcement-concrete bonding interaction, the embedded method with perfect bond between reinforcement and surrounding concrete was used. It was worth noting that the effects commonly associated with the reinforcement-concrete interface, such as bond slip and dowel action, were modelled indirectly by incorporating "tension stiffening" into the reinforced concrete model to approximate load transfer across cracks through the rebar (ABAQUS user's manual (2014)). To solve nonlinear problems, ABAQUS/Standard employs the Newton-Raphson method. Newton–Raphson equilibrium iterations provide convergence within tolerance limits at the end of each load increment for all degrees of freedom in the model. The Newton–Raphson approach was used to analyse the residual load vector, which was the difference between the internal forces (the loads corresponding to the element stresses) and the external applied loads. ABAQUS/Standard also ensures that the displacement correction was small in comparison to the total incremental displacement, and it was regularised so that both convergence checks (loads and displacements) must be satisfied before a solution is considered converged for that load increment.

6.4 LOADING AND BOUNDARY CONDITIONS

On top of the column, a constant axial load was initially applied. This was followed by a reverse cyclic load applied at the beam's tip to control displacement. The top end of the column was restrained by a rigid surface, which allows the end to behave as a pin, and the bottom end was restrained by a rigid surface, which allows the end to behave as a roller in the Y direction. The column's lateral displacement was limited by the pinned connection at the top, but it was free to rotate and elongate. The beam end was free to rotate and translate horizontally but restricted vertically. The loading and boundary condition of normal joint and retrofitted joint is shown in figure 6.4 and 6.5 respectively.

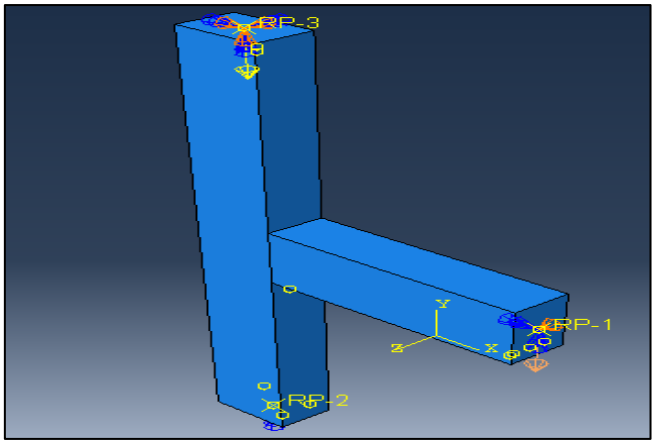

Figure 6.4 Loading and boundary conditions of joint in Abaqus

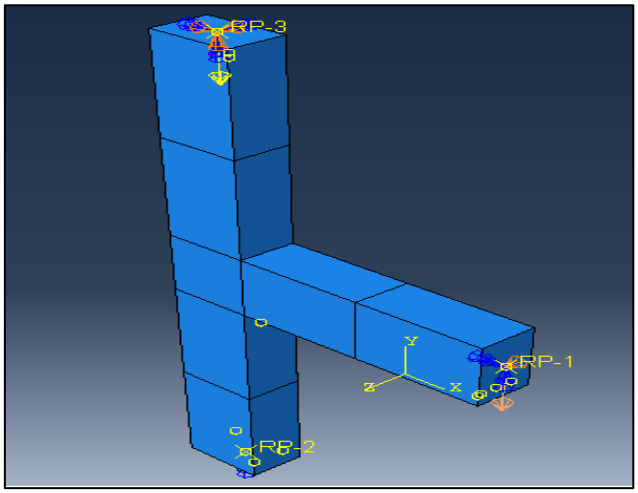

Figure 6.5 Loading and boundary conditions of CFRP retrofitted joint in Abaqus

6.5 MESH ARRANGEMENT

Meshing is essential in the engineering simulation process because it divides complex geometries into simple elements that can be used as distinct local approximations of the larger domain. The mesh arrangement for a model influences the simulation's accuracy, convergence, and speed. The meshing procedure consumes a significant portion of the time required to obtain simulation results. The better and more automated the meshing tools, the faster and more accurate the solution. Figures 6.6 and 6.7 show meshed model of a normal joint and a retrofitted joint respectively. For this study, a mesh size of 30 mm was used for concrete. Also, mesh size of 10 mm for reinforcement and mesh size of 8 mm for CFRP was used.

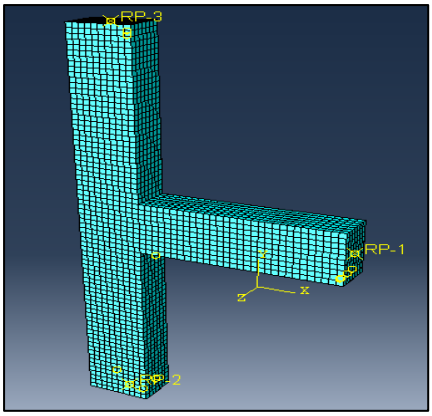

Figure 6.6 Meshed model of joint

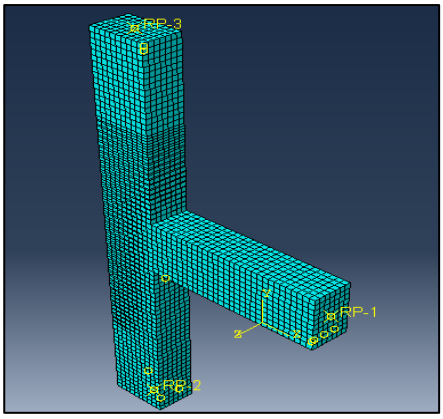

Figure 6.7 Meshed model of CFRP retrofitted joint

6.6 ANALYSIS AND VISUALIZATION

The analysis step comes after the initial step. Two analytical phases were developed for this investigation, one for the examination of axial loads and the other for reverse cyclic loads. In this work, nonlinear analysis was utilized. There was a maximum of 10000 increments inside each stage. The field output requirement was the response force and lateral displacement of the beam at the load application location. Over each phase, the load will change linearly with time. The analysis's findings were presented in the visualization module. This module obtains the output data that was requested in the step module. The X-Y plot was created to show the joint's displacement in relation to time and the applied load. Load was defined as a linear function of time in the produced plot. Thus, the load verses deflection graph may be created from the X-Y data. Load was defined as a linear function of time in the produced plot. Thus, the load verses deflection graph may be created from the X-Y data.

6.7 SUMMARY

The modelling for concrete, reinforcement and CFRP has been done separately. The concrete was represented by an eight-nodded linear brick element (C3D8R). To model main and transverse reinforcement, a 2-node linear 3-D truss element (T3D2) was used, whereas CFRP was modelled using a 4-noded shell element (S4R). The load displacement graphs for retrofitted models and normal beam column joint were developed. The graph showing the variation in stiffness degradation and cumulative energy dissipation with respect to drift ratio were also plotted. The results of the analysis were used to compare the performance of the models in terms of load carrying capacity, energy dissipation capacity, stiffness degradation, and ductility.

CHAPTER 7

RESULTS AND DSICUSSIONS

7.1 GENERAL

The numerical analysis on retrofitted beam column joint was conducted to study the improvement in load carrying capacity of retrofitted joint compared to that of a normal joint. The effect of parameters, namely number of layers of CFRP sheets and different orientations of CFRP sheets were studied and the results are discussed in the following sections.

7.2 EFFECT OF NUMBER OF LAYERS OF CFRP

The effect of number of layers of sheets was studied by considering one, two and three layers of CFRP sheets. Two different cases of fiber orientation were considered. They are unidirectional fibers and fiber orientation at 0° and 90°respectively.

7.2.1 Unidirectional fibers in CFRP sheets

In order to study the effect of number of layers of CFRP sheet on performance of beam column joint, beam column joint retrofitted with 1, 2 and 3 layers of CFRP sheets with unidirectional fibers were numerically analyzed and the results were compared to the load carrying capacity of normal joint. Deformed model of retrofitted joint with different layers of CFRP is shown in figure 7.1(a) to 7.1(c). Figure 7.2 represents the load displacement curve for beam column joint retrofitted with different number of layers of CFRP and that of a normal joint. It can be concluded from the graph that as the number of layers of CFRP sheet increases, the load carrying capacity of the joint also increases. Figure 7.3 shows the efficiency-displacement factor curve for retrofitted joint with different layers of CFRP with unidirectional fibers. The variation of efficiency and load factor curve was similar in all three cases and hence the result of analysis has been verified. The load carrying capacity of retrofitted beam column joint with 1, 2, and 3 layers of CFRP were higher than that of the normal joint. The improvement in the load carrying capacity of retrofitted beam column joint with 1, 2, and 3 layers of CFRP were 18%, 42% and 55 % higher than that of the normal beam column joint.

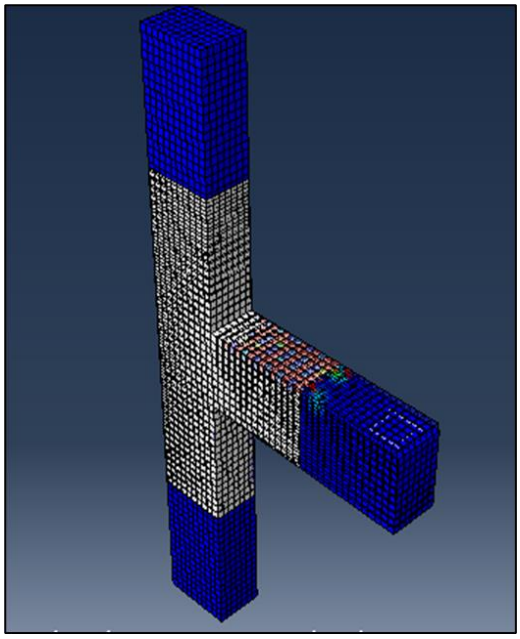

(a) One layer of CFRP

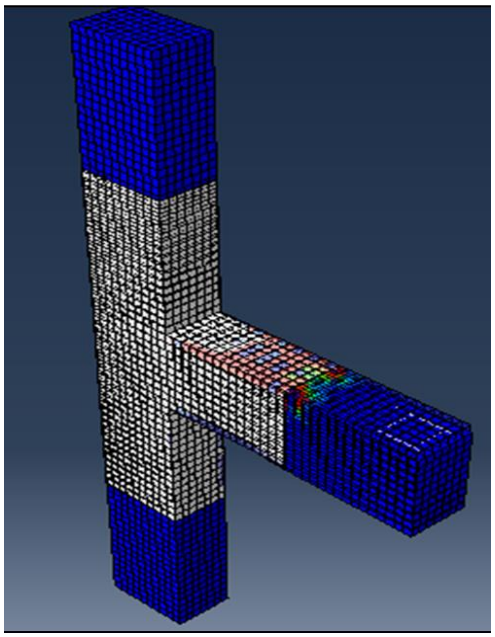

(b) Two layers of CFRP

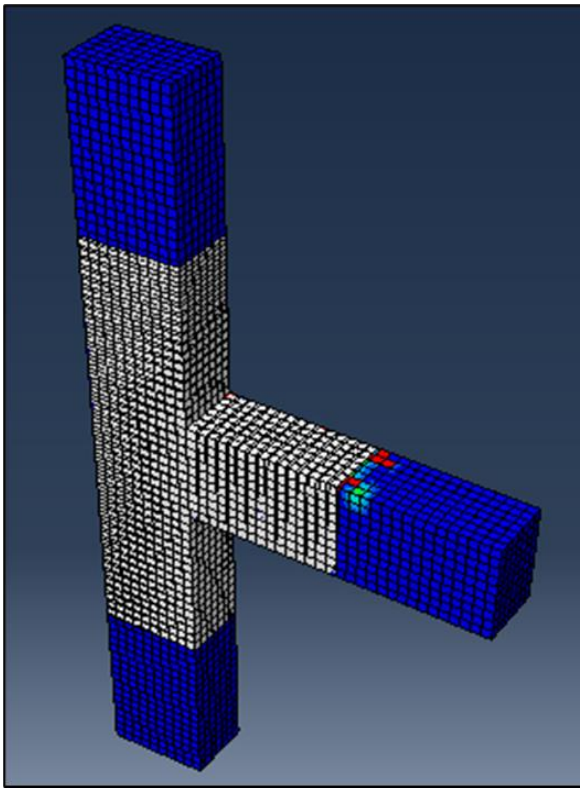

(c)Three layers of CFRP

Figure 7.1 Deformed model of unidirectional CFRP sheets retrofitted joint with: (a) 1 layer of CFRP, (b) 2 layers of CFRP and (c) 3 layers of CFRP

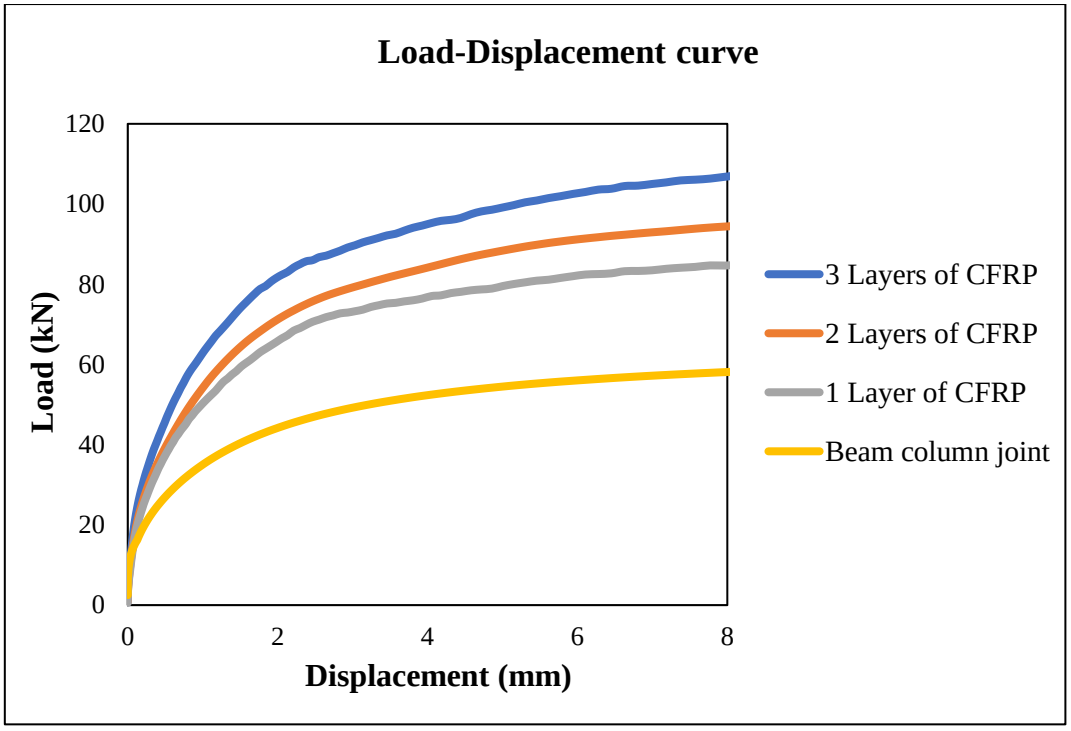

Figure 7.2 Load-displacement curve for retrofitted joint with different layers of CFRP with unidirectional fibers

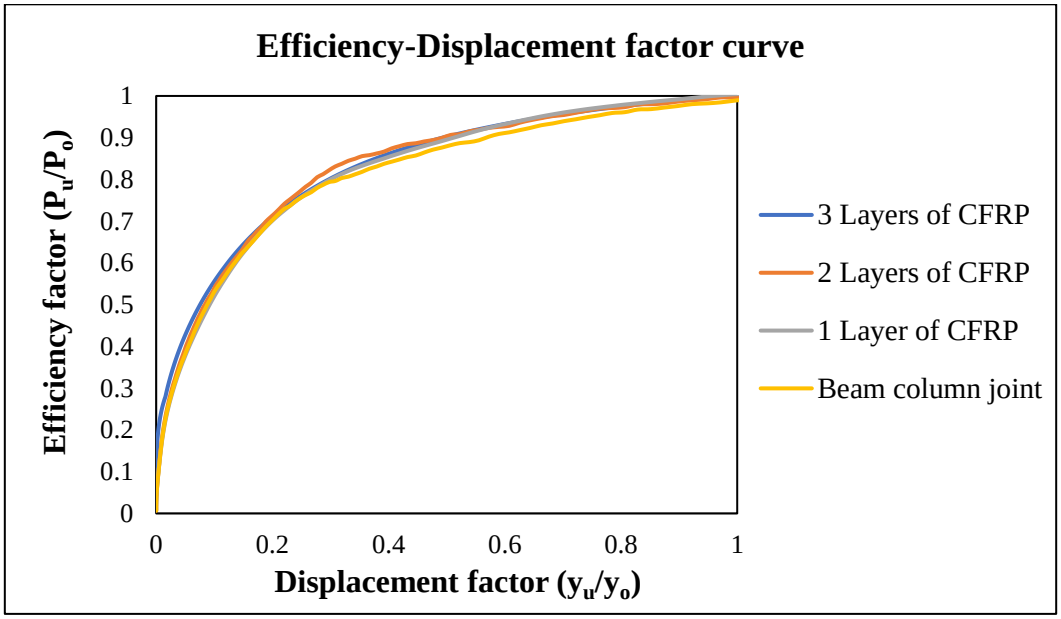

Figure 7.3 Efficiency-Displacement factor curve for retrofitted joint with different layers of CFRP with unidirectional fibers

7.2.2 Fibers are oriented at 0° and 90° in CFRP sheets

To investigate the effect of the number of layers of CFRP sheet with fibres oriented at 0° and 90° on beam column joint performance, beam column joints retrofitted with 1, 2, and 3 layers of CFRP sheets with fibres oriented at 0° and 90° in alternate layers

were numerically analysed and the results were compared to the load carrying capacity of a normal joint. Figure 7.4(a) to 7.4(c) depicts a deformed model of retrofitted joint with different layers of CFRP sheets. Figure 8.5 depicts the load displacement curve for a beam column joint retrofitted with fibres oriented at 0° and 90° in alternate layers of CFRP and that of a normal joint. The graph shows that as the number of layers of CFRP sheet increases, so does the load carrying capacity of the joint. The load carrying capacity of a retrofitted beam column joint with one, two, or three layers of CFRP was greater than that of a normal joint. The load carrying capacity of retrofitted beam column joints with 1, 2, and 3 layers of CFRP was 18%, 55%, and 89% higher than that of the standard beam column joint, respectively. As shown in figure 7.6, the variation of the efficiency factor and load factor curve for the retrofitted joint was similar in all three cases, indicating that the result was correct. The load displacement curve of unidirectional fibres and fibres oriented at 0° and 90° is shown in Figure 7.7, and all three cases of fibre orientation with 0° and 90° performed better than the unidirectional fibres in terms of load carrying capacity.

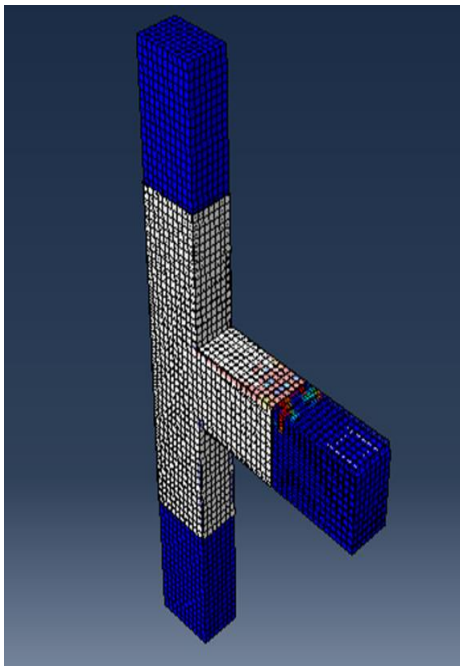

(a) One layer of CFRP

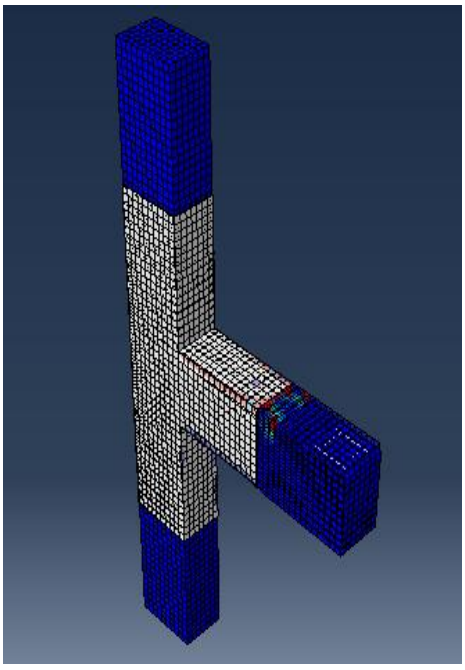

(b) Two layers of CFRP

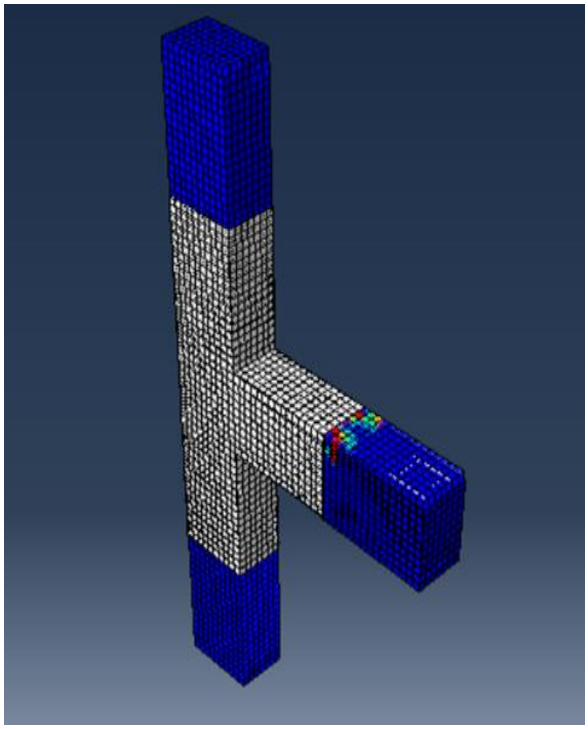

(c)Three layers of CFRP

Figure 7.4 Deformed model of retrofitted joint with fibers oriented at 0° and 90° in CFRP sheets with :(a) 1 layer of CFRP, (b) 2 layers of CFRP and (c) 3 layers of CFRP

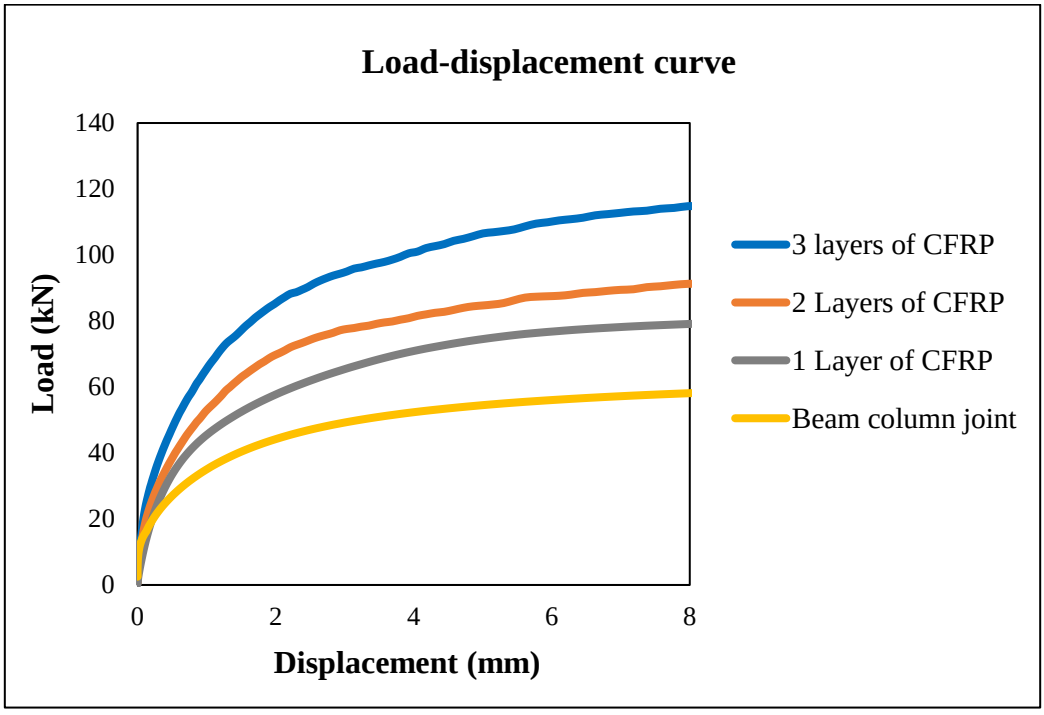

Figure 7.5 Load-displacement curve for retrofitted joint with CFRP sheets oriented with fibers at 0° and 90°

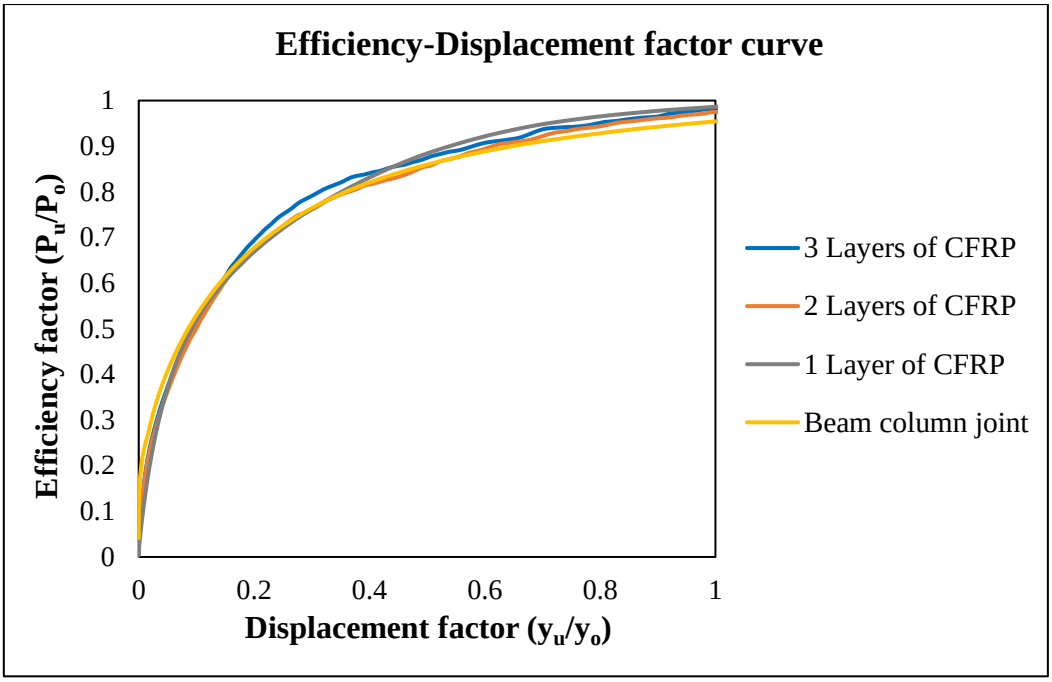

Figure 7.6 Efficiency-Displacement factor curve for retrofitted joint with CFRP sheets oriented with fibers at 0° and 90°

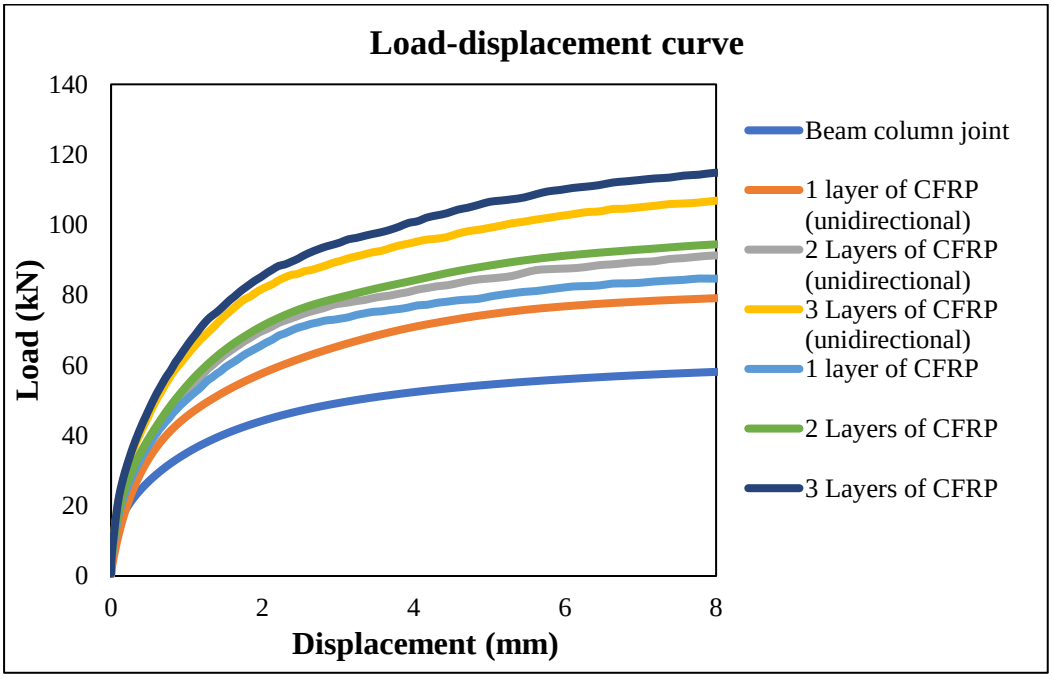

Figure 7.7 Load-displacement curve for retrofitted joint with unidirectional CFRP sheets and sheets with fibers oriented at 0° and 90°

7.3 EFFECT OF ORIENTATION OF CFRP SHEETS

To investigate the effect of CFRP sheet orientation on the performance of a beam column joint, three orientations of CFRP sheets were numerically analysed and the results were compared to the load carrying capacity of a normal joint. The different

orientations considered were X, L and C shaped sheets. In all the three cases, the area of CFRP used was same and is 1.7 m^2. Th main objective was to find the best orientation of CFRP for a given area of CFRP sheets. Figure 7.8 depicts a deformed model of a retrofitted joint with a different orientation of CFRP sheets. The load displacement curve for a beam column joint retrofitted with different orientations of CFRP and that of a normal joint was shown in figure 7.9. The graph shows that the X-shaped sheet had a higher load carrying capacity than the other two orientations. The load carrying capacity of the C-shaped orientation sheet was the lowest. The load carrying capacity of the retrofitted beam column joint with all three CFRP orientations were greater than that of the normal joint. The efficiency-displacement factor curve for a retrofitted joint with different layers of CFRP with unidirectional fibres is shown in Figure 7.10. The variation of the efficiency and load factor curves is similar in all three cases, indicating that the result was correct. The load carrying capacity of retrofitted beam column joints with X shape, L shape, and C shape CFRP sheets were 83%, 62%, and 43% higher than that of the normal beam column joint, respectively.

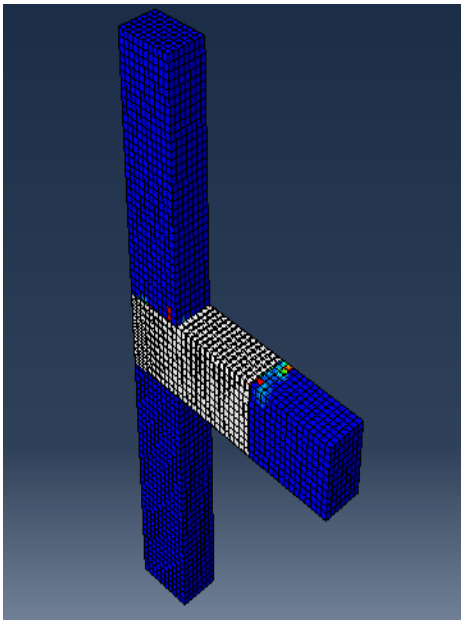

(a) C shaped sheet

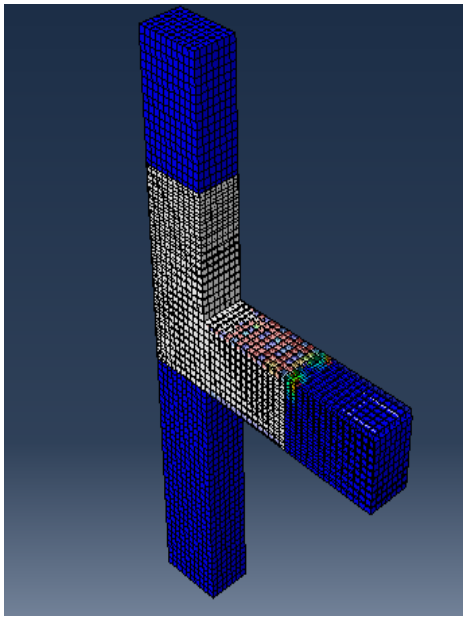

(b) L shaped sheet

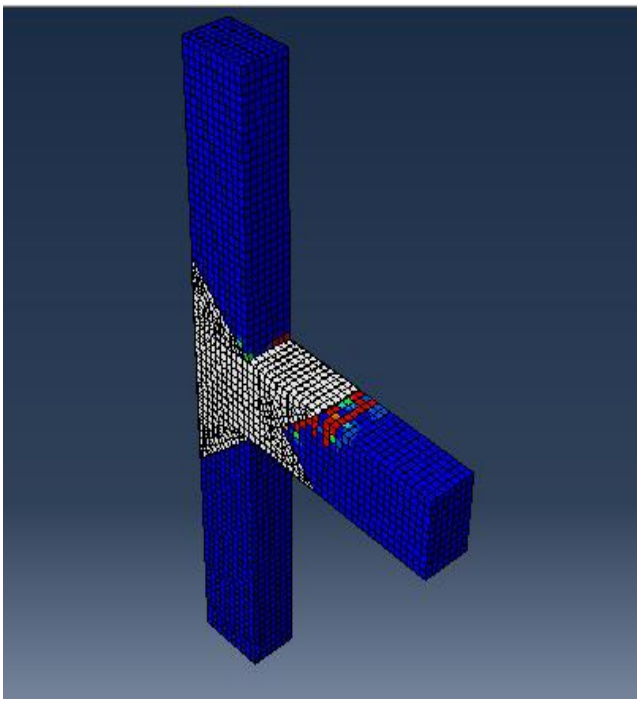

(c) X shaped sheet

Figure 7.8 Deformed model of retrofitted joint with orientations with :(a) C shaped sheet, (b) L shaped sheet and (c) X shaped sheet

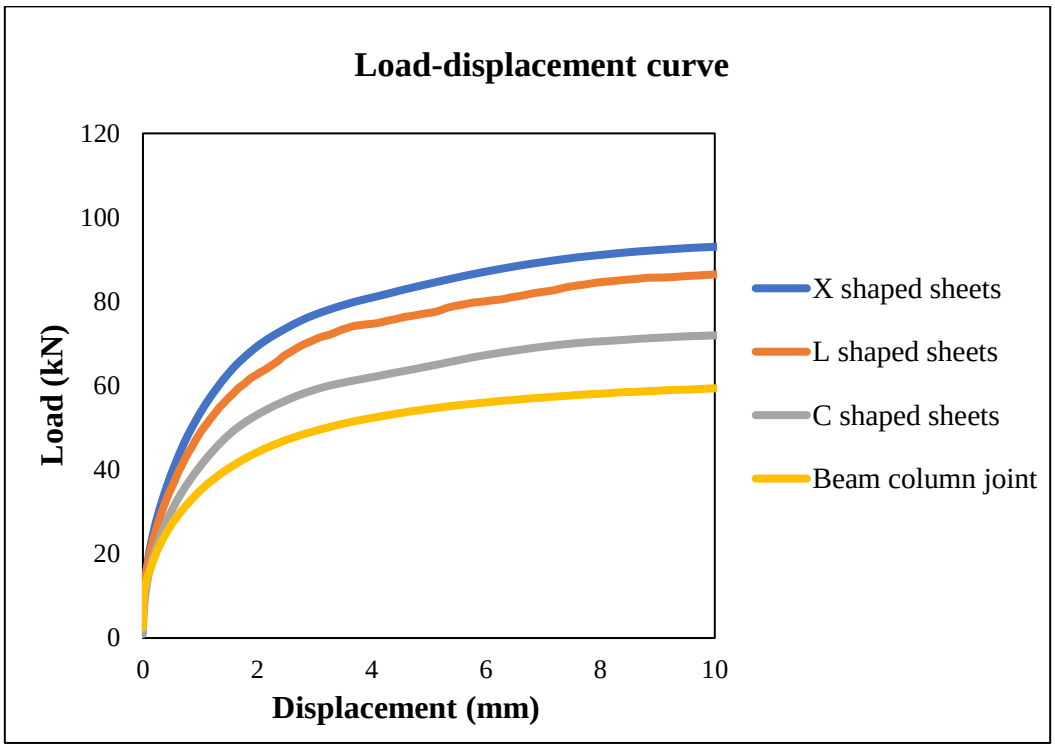

Figure 7.9 Load-displacement curve for retrofitted joint with different orientations of CFRP sheets

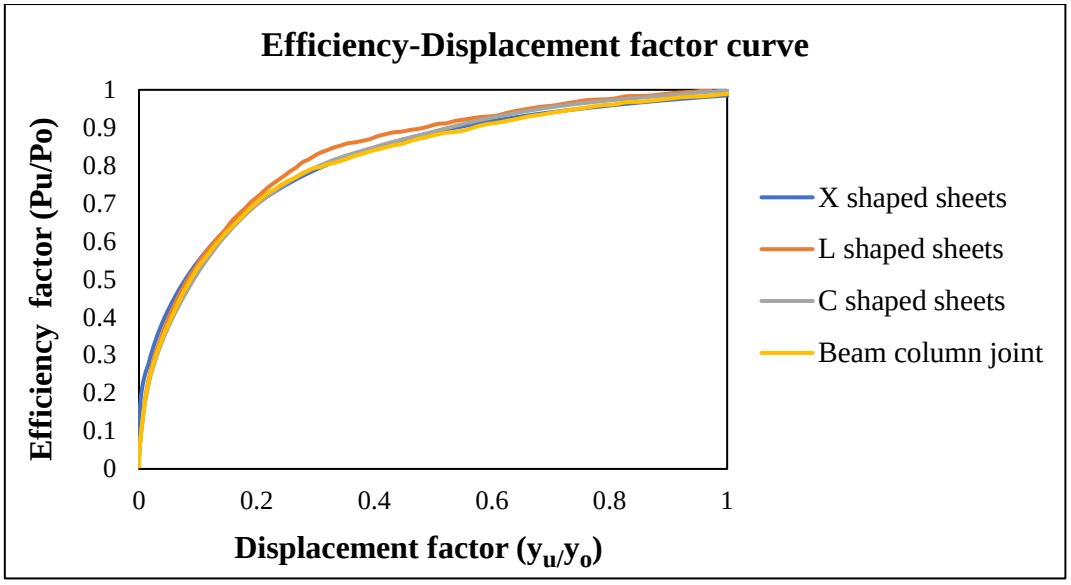

Figure 7.10 Efficiency-Displacement factor curve for retrofitted joint with different orientations of CFRP sheets

7.4 FIRST CRACK LOAD

The first crack load of a beam column joint was the load at which the crack begins to form. Figure 7.11 depicts the instant at which a crack developed in a retrofitted beam column joint with one layer of CFRP with unidirectional fibres. Figure 7.12 depicts the deformed model retrofitted with 1-layer CFRP after complete crack formation. It is very clear from the figure that the cracks developed in the beam region and also it didn't destroy the CFRP layer. Hence the model is safe even after complete formation of cracks. Abaqus calculates the first crack load by comparing the deformed model and the load versus time curve as shown in figure 7.13. The first crack load for a joint with three layers of CFRP was 43.35 kN, and the corresponding drift ratio was 3.75% for unidirectional fibres. The first crack load was greater for joints retrofitted with three layers of CFRP sheets than for models with fibres oriented at 0° and 90°. Among the models with fibres oriented at 0° and 90°, the joint retrofitted with 3 layered CFRP sheets has a higher first crack load. The value was 62.35 kN, and the drift ratio was 5.25%. In the case of models with different orientations, the X shaped sheet had the highest first crack load of 34.27 kN and with the lowest drift ratio of 2.93%, while the C shaped sheet had the lowest first crack load. The strong bond formed between the injected epoxy and the concrete resisted crack propagation within the concrete as well as the initially undamaged concrete of the strengthened specimen. Table 7.1 gives the first crack load and corresponding drift ratio of all models. The failure of the retrofitted

specimens shifted from columns to beams due to the strengthening of beam-column joints, as evidenced by the cracking pattern of the specimens shown in figure 7.12.

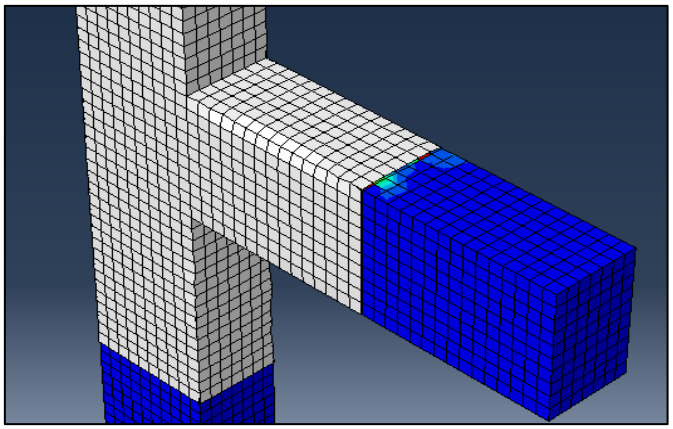

Figure 7.11 Crack initiation in retrofitted joint

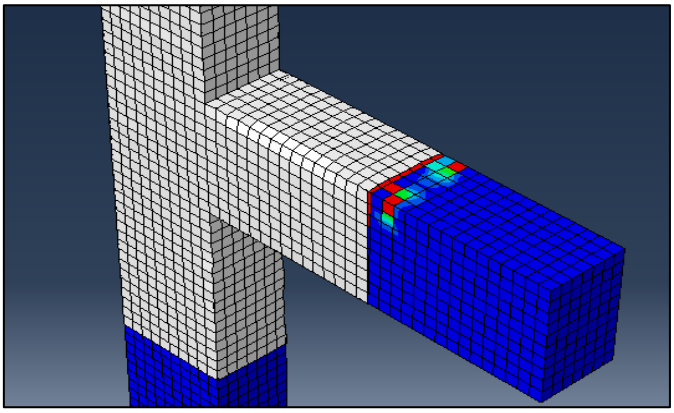

Figure 7.12 Complete formation of cracks in retrofitted joint

Table 7.1 First crack load and drift ratio of beam column joint models

Specimen	**First crack load (kN)**	**Drift ratio (%)**
Beam column joint	20.45	0.26
(a) Unidirectional fibers		
1 layer of CFRP	27.49	1.85
2 layers of CFRP	36.75	3.23
3 layers of CFRP	43.45	3.75
(b) Fibers are oriented at 0° and 90°		
1 layer of CFRP	52.54	4.13
2 layers of CFRP	57.94	4.56
3 layers of CFRP	62.35	5.25
(c) Different orientation of CFRP sheets		
C shaped sheet	24.37	1.33
L shaped sheet	31.79	2.43
X shaped sheet	34.27	2.93

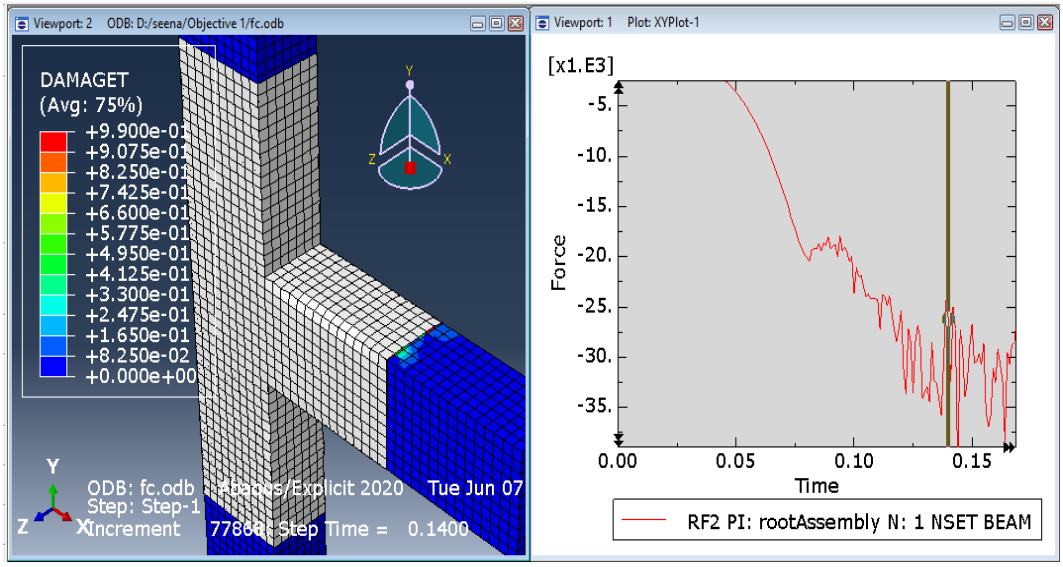

Figure 7.13 Determination of first crack load from ABAQUS

7.5 COMPARISON OF MODELS IN TERMS OF DUCTILITY, ENERGY DISSPIATION CAPACITY AND STIFFNESS DEGRADATION

7.5.1 Hysteresis loop

The investigation of the load-displacement hysteretic response of specimens is critical to evaluate their seismic performance. Ductility and energy dissipation are two fundamental parameters of structural performance under lateral loads which could be evaluated using hysteretic plot. Hysteretic behaviours such as capacity, strength deterioration, and stiffness degradation can be used to evaluate the cyclic performance characteristics of beam column joints. Figure 7.14 depicts the cyclic loading history applied to the models. Positive hysteretic plots represent push values, while negative region curves represent pull values. The hysteretic curves differ significantly in the push and pull directions.

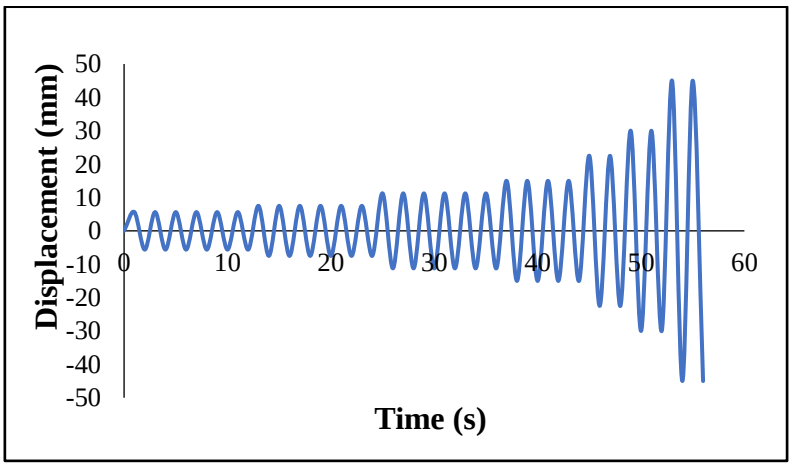

Figure 7.14 Cyclic loading history

The exterior joint's hysteretic behaviour was investigated in terms of ductility, energy dissipation capacity, and stiffness degradation. Figures 7.16 to 7.18 show that the ultimate loads and deformation capacities for models retrofitted with CFRP were significantly higher than those shown in figure 7.15 for normal beam column joint. This was primarily due to the increased joint confinement caused by externally bonded CFRP sheets. In Figures 7.16 and 7.17, the increase in ultimate load and deformation capacity was proportional to the number of layers of CFRP. The increase in ultimate load and deformation capacity for retrofitted specimens with three layered CFRP with unidirectional fibres, as shown in figure 7.16(c), was greater than for those with two layers and one layer, as shown in figures 7.16(a) and 7.16(b). The area of the loop was stable under both push and pull loads during the elastic stage. Following that, the cracking stage began, causing stiffness degradation in the specimen as the area of the loop increased with each loading cycle. This reduction could be attributed to progressive loading at each stage. Figure 7.17(c) shows that the three-layered CFRP with fibres oriented at 0° and 90° had the highest stiffness and strength capacity in both positive and negative loading, when compared to the models shown in figures 7.17(a) and 7.17(b). These desirable responses were caused by shifting plastic stresses away from the column face and joint core to the beam, resulting in the beam's ductile flexural hinging. In the case of different CFRP sheet orientations, the retrofitted model with an X-shaped sheet orientation, as shown in figure 7.18(c), performed slightly better than the model with an L-shaped sheet orientation, as shown in figure 7.18(b). As shown in figure 7.18(a), the performance of C-shaped CFRP sheet orientation for ultimate load carrying capacity was lower when compared to the other two orientations of retrofitted models. Furthermore, all of the repaired joints demonstrated an increase in load-carrying capacity over the normal beam column due to the retrofitting orientation of CFRP sheets. The load and its corresponding displacement were calculated from these hysteretic and envelope curves. In all models, the load-displacement responses of each specimen were nearly symmetrical in both the positive and negative directions. A comparison of the hysteretic curves of all models' specimens revealed a significant drop in lateral strength after reaching peak load in each cycle repetition. This could be attributed to shear damages, which were primarily concentrated in the joint area, as well as concrete crushing under higher loads. All of the retrofitted joint's hysteretic load-displacement loops demonstrated a significant improvement in horizontal load and displacement behaviour.

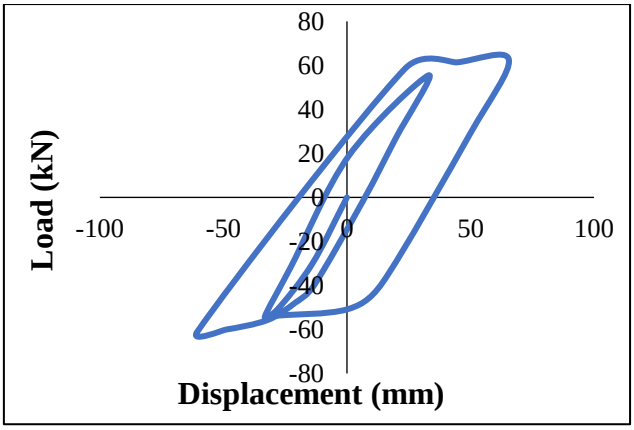

Figure 7.15 Load-displacement hysteretic response of normal beam column joint

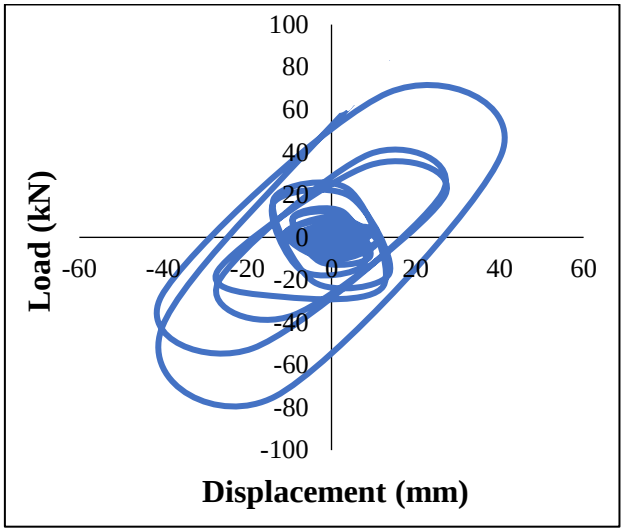

(a) One layer of CFRP

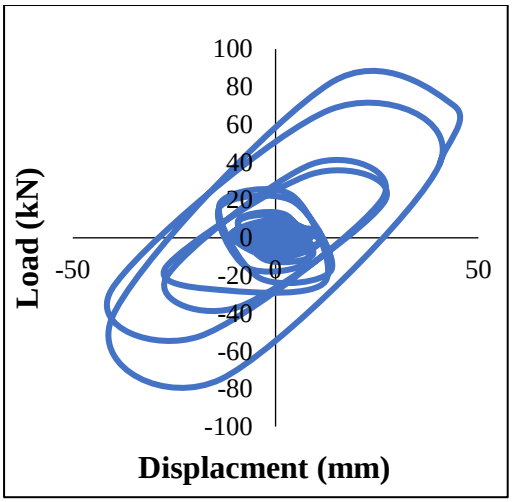

(b) Two layers of CFRP

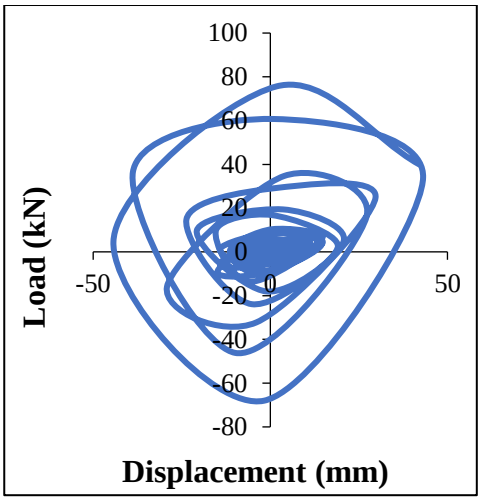

(c) Three layers of CFRP

Figure 7.16 Load-displacement hysteretic response of unidirectional CFRP sheets retrofitted joint with: (a) 1 layer of CFRP, (b) 2 layers of CFRP and (c) 3 layers of CFRP

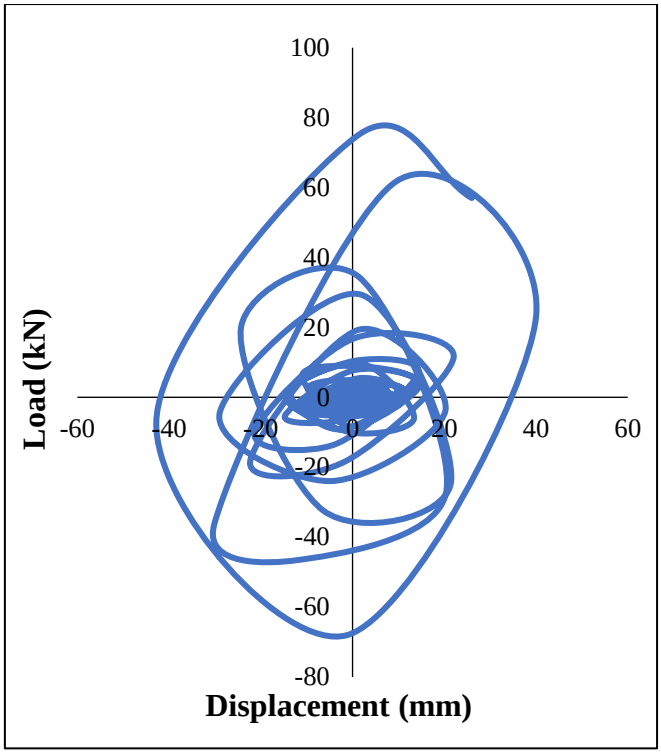

(a) One layer of CFRP

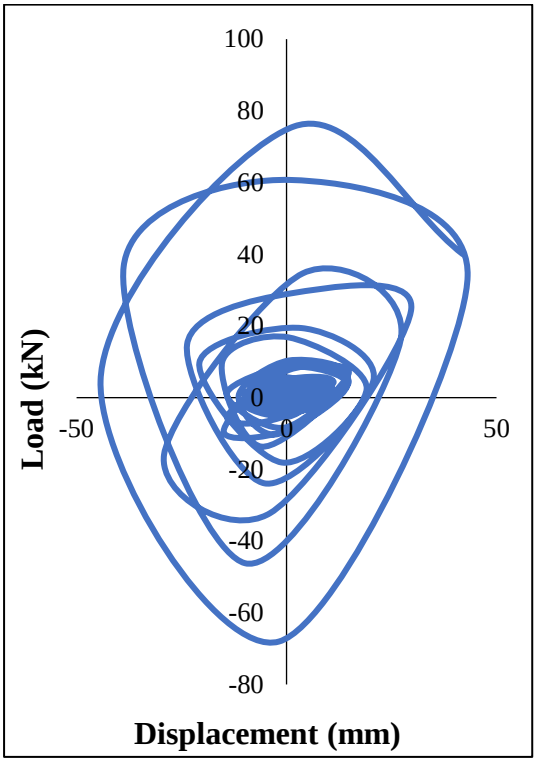

(b) Two layers of CFRP

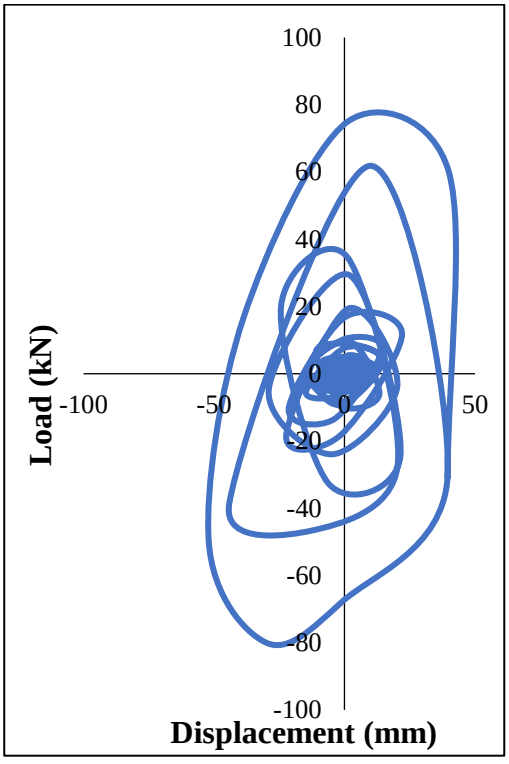

(c) Three layers of CFRP

Figure 7.17 Load-displacement hysteretic response of retrofitted joint with fibers oriented at 0° and 90° in CFRP sheets with :(a) 1 layer of CFRP, (b) 2 layers of CFRP and (c) 3 layers of CFRP

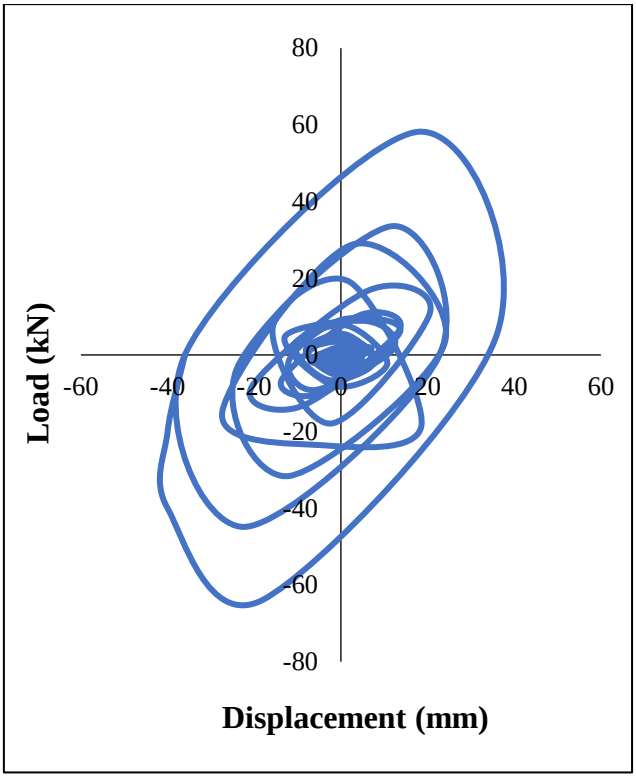

(a) C shaped sheet

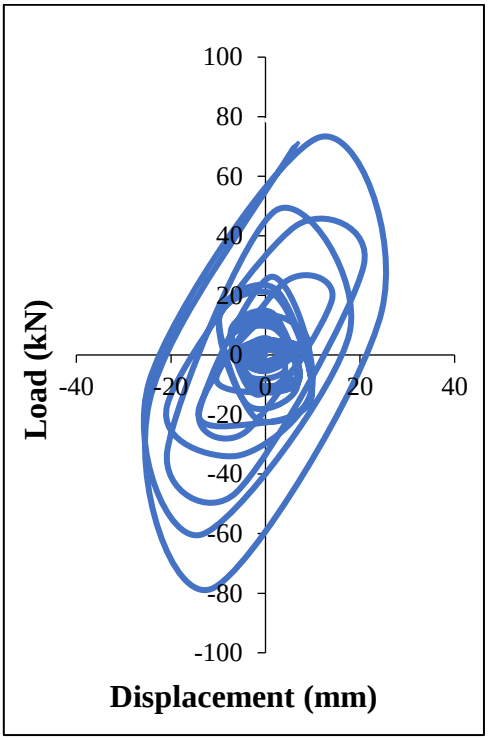

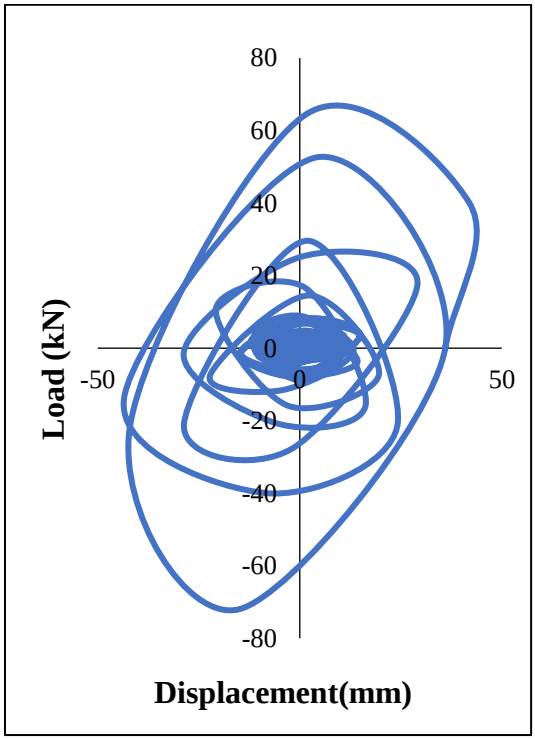

(b) L shaped sheet

(c) X shaped sheet

Figure 7.18 Load-displacement hysteretic response of retrofitted joint with orientations :(a) C shaped sheet, (b) L shaped sheet an (c) X shaped sheet

7.5.2 Ductility

Ductility is defined as a structures and its element's ability to withstand massive inelastic deformation without significantly reducing strength. During inelastic cyclic deformations, ductile structures can dissipate hysterically large amounts of energy. Ductility is an important parameter for quantifying the seismic behaviour of a structure or element. The ductility of a building is an important factor in earthquake resistance. Ductility is defined as the ability of structural members to undergo large deformations in the plastic region while maintaining their loading capacity (Sarkar et al., 2007). The performance of the retrofitted models was compared in this section in terms of ductility. A ductile structure can dissipate significant amounts of energy in a hysteretic mode during inelastic cyclic motions. The displacement ductility was defined as the maximum displacement divided by the yield displacement. Table 7.2 shows the maximum and yield displacement values, as well as the ductility of the numerically analysed models. It can be concluded that all retrofitted joints had good seismic performance. Fang et al. (2019) defined displacement ductility factor (μ) as the ratio of ultimate displacement (d_u) to displacement at yield (d_y), and is given as

$$\mu = d_u / d_y$$

Clearly, the use of CFRP sheets increased the ductility of all retrofitted models when compared to the normal beam column joint. In the case of a joint retrofitted with unidirectional CFRP fibres, the retrofitted specimen with three layers of CFRP had the highest ductility factor. Table 7.2 gives the displacement ductility factor values of all the models. The retrofitted models with three layers showed the greatest improvement in ductility in both cases of unidirectional fibres and fibres oriented at 0° and 90°. Among the different orientations of CFRP sheets, C-shaped wrapping was not as effective as L-shaped and X-shaped in improving both the capacity and ductility of the joint. The X-shaped sheets produced the best joint performance in terms of strength and ductility. The ductility of retrofitted beam column joints with 1, 2, and 3 layers of CFRP with unidirectional fibres were 75.56%, 83.21%, and 92.23% higher than that of the normal beam column joint, respectively. The improvement in ductility of 1, 2, and 3 layers of CFRP retrofitted model with fibres oriented at 0° and 90° were 75.56 %, 83.21 %, and 92.23 % compared to that of the normal beam column joint, respectively. In the case of models retrofitted with different orientations of CFRP, the ductility of retrofitted

beam column joints with C shape, L shape, and X shape sheet of CFRP were 21.88 %, 45.57 %, and 57.72 % higher than that of the normal beam column joint, respectively. Table 7.2 gives the displacement ductility factor values of all the models. All the retrofitted models showed improvement in ductility compared to that of normal joint.

Table 7.2 Displacement ductility factor for models

Specimen	**Displacement at yield (mm)**	**Displacement at maximum load (mm)**	**Ductility factor**	**% Variation**
Beam column joint	1.50	10	6.67	-
(a) Unidirectional fibers				
1 layer of CFRP	1.65	18	10.91	63.56
2 layers of CFRP	1.74	21	12.07	80.95
3 layers of CFRP	1.82	23	12.63	89.35
(b) Fibers are oriented at 0° and 90°				
1 layer of CFRP	1.70	19	11.17	75.56
2 layers of CFRP	1.80	22	12.22	83.21
3 layers of CFRP	1.95	25	12.82	92.23
(c) Different Orientation of CFRP sheets				
C shaped sheet	1.60	13	8.13	21.88
L shaped sheet	1.75	17	9.71	45.57
X shaped sheet	1.90	20	10.52	57.72

7.5.3 Energy dissipation capacity

Energy dissipation capacity is a vital parameter in assessing the seismic behaviour of structures under lateral loads. Energy dissipation in concrete structures includes energy dissipated by steel reinforcements, energy dissipated during crack development, and friction between crack surfaces. Certain structural members can withstand large deformations (Mirza et al., 2010). As a result, they are the ones who dissipate energy and reduce the effects of seismic forces on the structure. When a building is subjected

to a severe earthquake, a building with a higher energy dissipation capability can absorb more energy, resulting in the building collapsing later. The area under the cycle of a specimen's cyclic response is defined as the energy dissipated in each cycle. Energy dissipation as a result of inelastic action. The area enclosed inside a hysteretic loop equals the energy dissipation due to inelastic action in that cycle (Kotsouvou et al., 2012). The greater the energy dissipation, the fatter the cycle. The sum of energy dissipated in successive loops throughout the test is known as cumulative energy dissipation. Figures 7.19-7.21 depict the cumulative energy dissipation versus drift ratio for normal and retrofitted specimens. Table 7.3 displays the total energy dissipation capacity of all beam column joint models. All of the retrofitted models outperformed the normal beam column joint in terms of energy dissipation, demonstrating that the retrofitting strategy is effective. After a 1.6 % drift ratio, energy dissipation began to rise significantly for all three joints when retrofitted with CFRP sheets with unidirectional fibres, as shown in figure 7.19. This demonstrates that CFRP wrapping is an effective method for preserving and increasing the energy dissipation capacity of heavily damaged concrete elements. When 1.8 % drift ratio was applied to CFRP with fibres oriented at 0° and 90°, as shown in figure 7.20, after that the cumulative energy dissipation increases significantly when compared to normal beam column joint. In the case of retrofitted models with different orientations, as shown in figure 7.21, energy dissipation of all three models and normal beam column joints was similar at the first loading cycle, specifically until at drift ratio of 1.9 %. However, in later loading cycles, the energy dissipation of the X shaped sheet orientation was greater than that of the L and C shaped orientations. This comparison demonstrated once more that CFRP strengthening patterns could improve the seismic behaviour of specimens with completely fat hysteretic loops during large lateral displacements. At a drift ratio of 4.8 %, the improvement in energy dissipation for three layers of CFRP sheets with unidirectional fibres was 11.11 %, and 12.25 % higher than for two layers and one layer respectively. Three-layered CFRP sheets with fibres oriented at 0° and 90° dissipated 10% and 15% more energy than two-layered and one-layered retrofitted joints, respectively at a drift ratio of 4.8 %. At a drift ratio of 4.8%, the X-shaped sheet dissipated more energy than the L-shaped and C-shaped sheets by 18.86 % and 13.33 %, respectively. It was observed that joints rehabilitated using the proposed strengthening system dissipate more energy than the normal when subjected to large lateral displacements of other structural members, ensuring the structure's safety.

Table 7.3 Total energy dissipation capacity of models

Specimen	Total Energy Dissipation Capacity (kNm)
Beam column joint	6.33
(a) Unidirectional fibers	
1 layer of CFRP	7.97
2 layers of CFRP	8.65
3 layers of CFRP	8.96
(b) Fibers are oriented at 0° and 90°	
1 layer of CFRP	9.34
2 layers of CFRP	10.22
3 layers of CFRP	11.42
(c) Different Orientation of CFRP sheets	
C shaped sheet	7.26
L shaped sheet	7.84
X shaped sheet	8.12

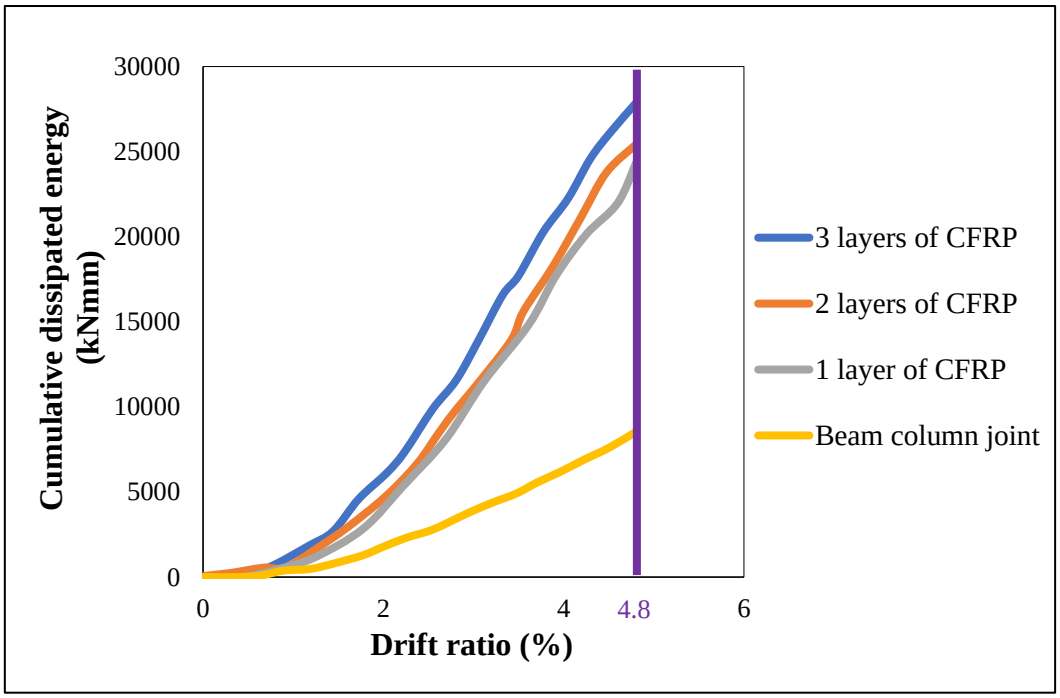

Figure 7.19 Cumulative energy dissipation against drift ratio for retrofitted joint with different layers of CFRP with unidirectional fibers

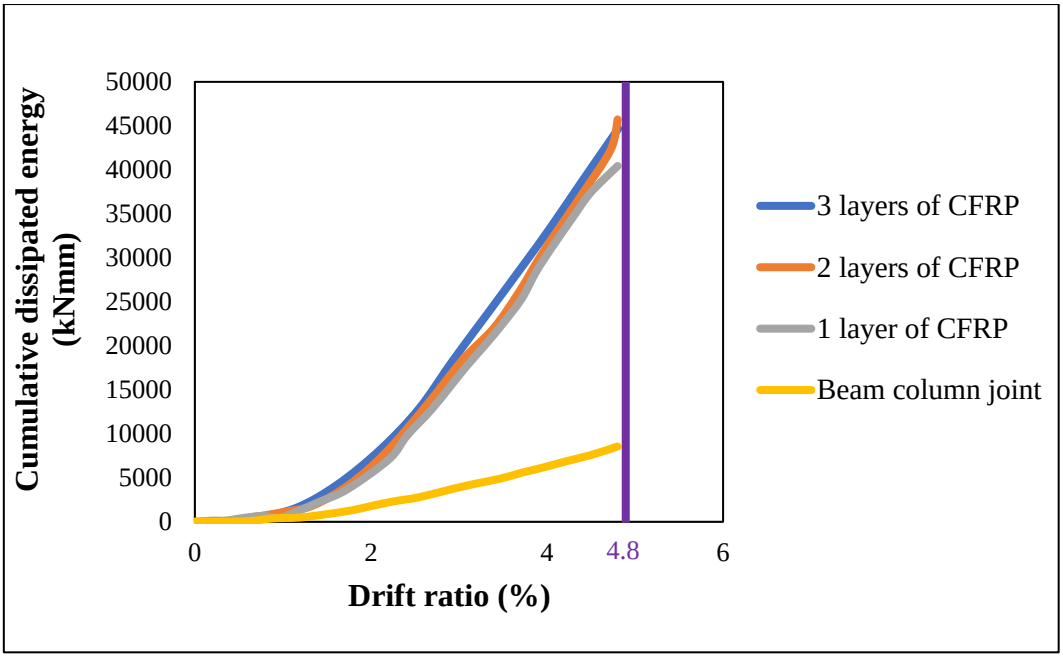

Figure 7.20 Cumulative energy dissipation against drift ratio for retrofitted joint with CFRP sheets oriented with fibers at 0° and 90°

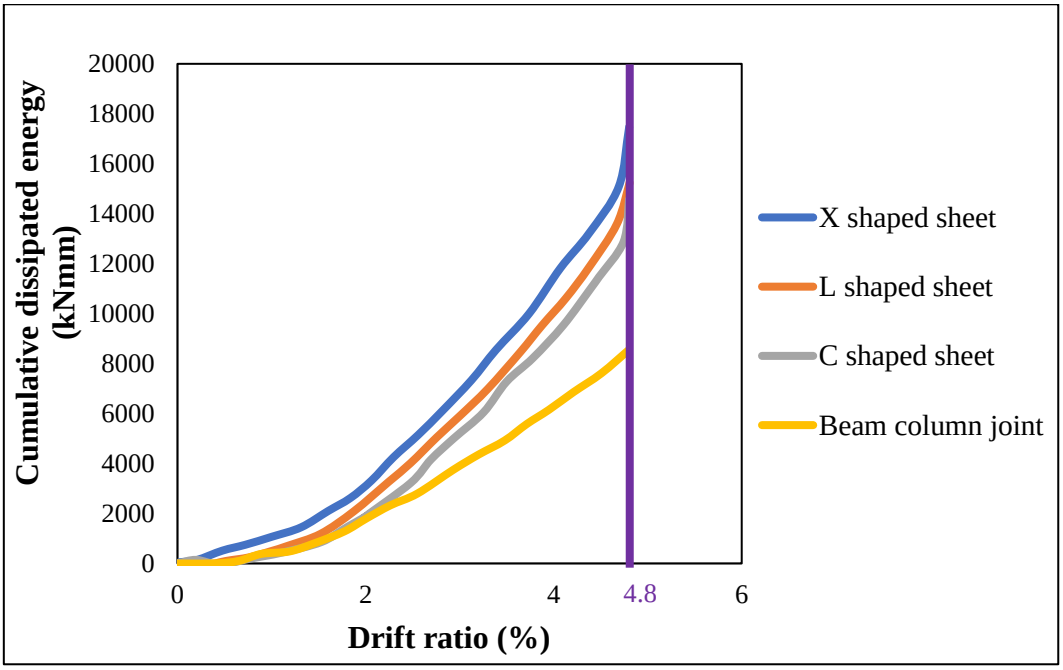

Figure 7.21 Cumulative energy dissipation against drift ratio for retrofitted joint with different orientation of CFRP sheets

7.5.4 Stiffness degradation

Stiffness degradation refers to the loss of stiffness as the structure's lateral movement increases. In other words, as the material of the specimen degrades with increasing load, the required force for a given displacement decreases. Flexural and shear cracks, shear

deformation of the connection core, loss of cover, concrete nonlinear behaviour, yielding of longitudinal rebars, concrete compression failure, longitudinal rebar slippage, failure or buckling of longitudinal steel, and second-order forces all erode the stiffness of a concrete structure (Venkatesan et al., 2016). The low rate of strength degradation is critical for RC structures in moderate earthquakes, where some damage to non-structural elements is permitted, but structural elements must have sufficient strength to remain elastic and avoid damage. The increased initial stiffness and lower rate of stiffness degradation will improve the behaviour of the beam column joint during an earthquake. In general, as the cycle numbers increase, the stiffness of the beam column joint decreases gradually. The secant stiffness degradation of the beam column joints is used to calculate the secant stiffness in each cycle. The stiffness degradation method as defined by Pohoryles et al. (2018) entails plotting the horizontal load-displacement hysteretic loop envelopes of each joint, and then calculating the secant stiffness for each cycle by dividing the sum of the maximum pushing and pulling loads by the sum of the maximum pushing and pulling corresponding displacements (the slope of the line between the maximum pulling and pushing and loads). As a result, at each drift ratio, the joint cyclic stiffness (K_i) is defined as the slope of the line connecting the maximum points of the first reversal cycle in the lateral load-displacement response, which can be expressed as follows:

$$K_{i=} (P_i^{+} - P_i^{-})/(d_i^{+} - d_i^{-})$$

where Pi and di are the maximum load and corresponding displacement in either the positive or negative direction. Table 7.4 shows the initial stiffness value for each model. Figures 7.22 -7.24 show the stiffness degradation versus drift ratio for various retrofitting scenarios with CFRP sheets. In the case of CFRP with unidirectional fibres, as shown in figure 7.22, retrofitted specimens with one layer and two layers had almost the same initial stiffnesses as the normal beam column joint. This is due to the fact that the retrofitted specimen was created by externally bonding the CFRP sheets to an undamaged concrete specimen. Furthermore, these specimens degrade at a slower rate than control specimens. This demonstrates the effectiveness of CFRP strengthening for joints. All retrofitted specimens in the case of CFRP retrofitted models with fibres oriented 0° and 90° showed higher initial stiffness compared to that of a normal beam column joint, as shown in figure 7.23. Furthermore, figure 7.24 shows that for a given

type of orientation, X shaped sheets have higher stiffness than L shaped and C shaped CFRP sheets. During the loading course, all retrofitted specimens produced a higher instantaneous rate of stiffness than the normal beam column joint. Although significant stiffness reductions were observed with crack development, the stiffness reduction for retrofitted models was less than that of a normal beam column joint. Because of the first crack, there was a significant decrease in secant stiffness values for normal joints. The sharp decrease in secant stiffness values for normal joints was caused by the first crack forming during the initial stages of loading as a result of joint critical reinforcement details, which caused concrete strength reduction and softening. Furthermore, a lower rate of degradation indicates that the structure was more ductile. Because the CFRP composite acted as a very effective confinement and prevented the formation of main cracks to the joint-column region, the stabilised reduction in secant stiffness values was clearly visible in strengthened joints. Furthermore, the CFRP strengthening technique significantly increased the initial secant stiffness of the joints.

Table 7.4 Initial stiffness of models

Specimen	**Initial Stiffness (kN/mm)**
Beam column joint	2.8
(a) Unidirectional fibers	
1 layer of CFRP	3.6
2 layers of CFRP	3.8
3 layers of CFRP	4.2
(b) Fibers are oriented at 0° and 90°	
1 layer of CFRP	4.6
2 layers of CFRP	5.6
3 layers of CFRP	6.4
(c) Different orientation of CFRP sheets	
C shaped sheet	3.2
L shaped sheet	3.5
X shaped sheet	3.8

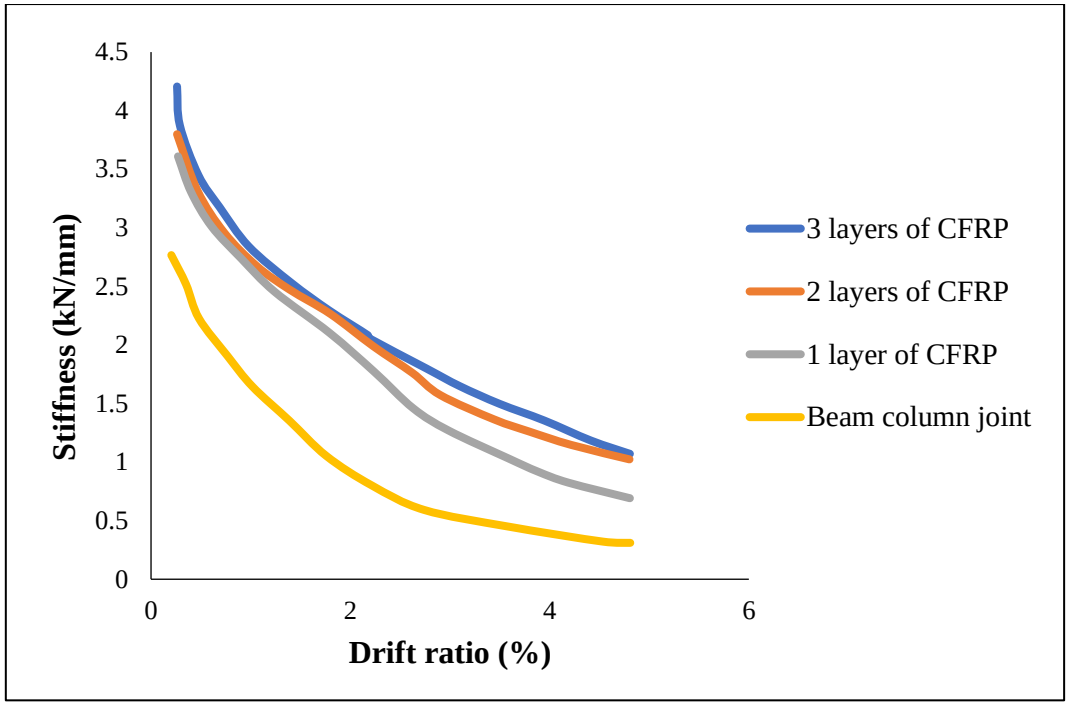

Figure 7.22 Stiffness degradation against drift ratio curve for retrofitted joint with different layers of CFRP with unidirectional fibers

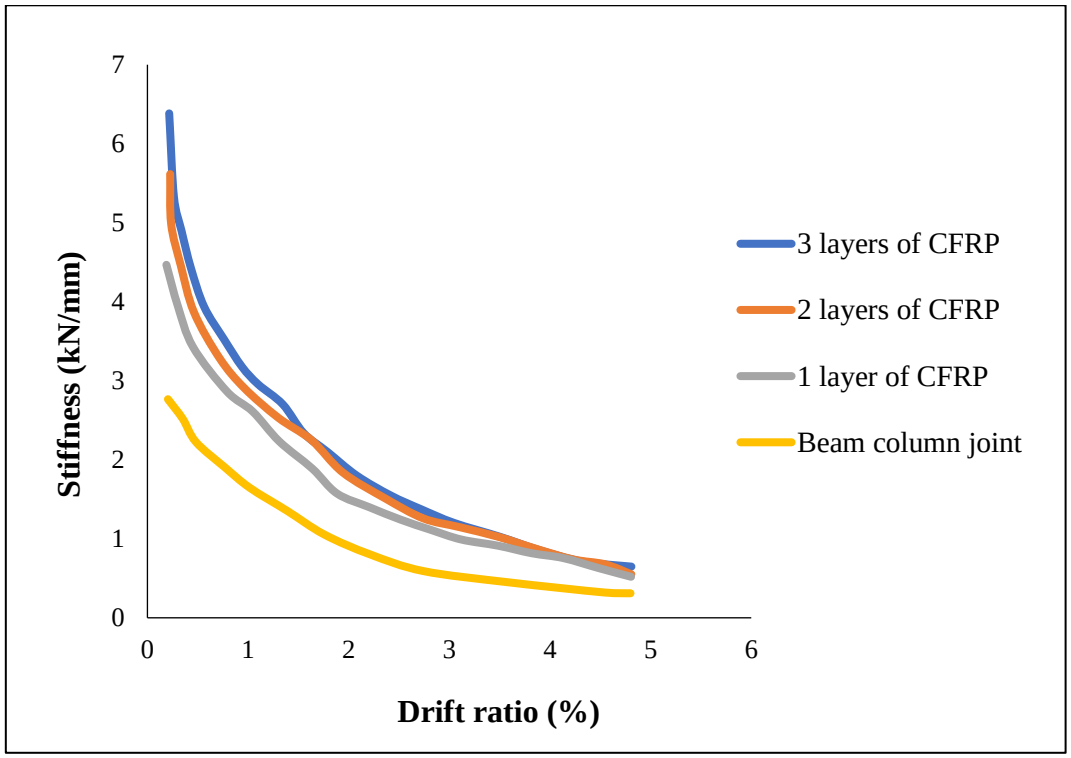

Figure 7.23 Stiffness degradation against drift ratio curve for retrofitted joint with CFRP sheets oriented with fibers at 0° and 90°

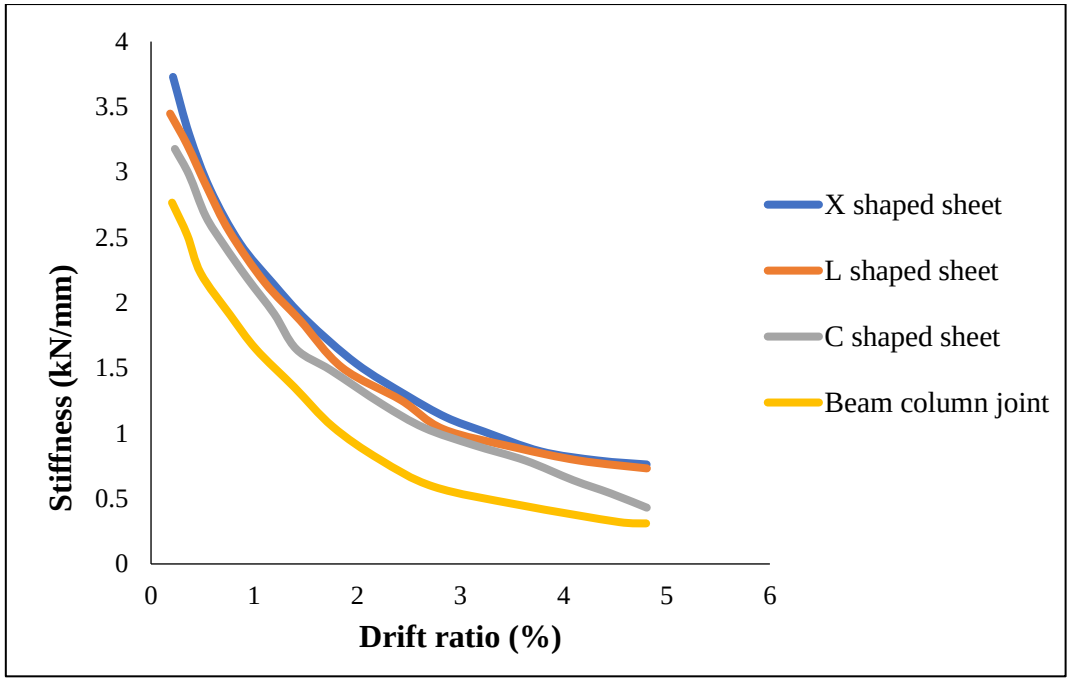

Figure 7.24 Stiffness degradation against drift ratio curve for retrofitted joint with different orientation of CFRP sheets

7.6 SUMMARY

In this chapter, the results of analysis were discussed in detail. The effect of number of layers with different orientation of CFRP was analyzed. Along with that the best orientation for a given area of CFRP sheets was also obtained. The improvement in load carrying capacity of retrofitted models with respect to that of normal joint was obtained from the load displacement curve. The hysteresis curve of all models was plotted to obtain the variation in energy dissipation capacity. Also, the ductility and stiffness degradation of all models were obtained and their performance were evaluated by comparing them with the performance of normal beam column joint.

CHAPTER 8

SUMMARY AND CONCLUSIONS

8.1 GENERAL

Beam column joint behavior is complex and critical for overall structural behavior. Beam-column connections are currently a major concern in structural engineering due to structural deficiencies caused by a combination of factors such as failing to consider seismic design and detailing requirements. Beam-column connections that lack such performance can be upgraded to the aforementioned level by repairing them with Carbon Fiber Reinforced Polymer (CFRP) composites. This study focused on the behavior of CFRP retrofitted exterior beam-column joint subjected to constant axial load and reverse cyclic load. Abaqus is the software application used in this study for modelling and analysis. For parametric study, the orientation and number of layers of CFRP sheet were analyzed.

8.2 SUMMARY

Numerical analysis of normal beam column joint and CFRP retrofitted beam column joint had been done using Abaqus software. The parameters studied were the number of layers of CFRP sheets and different orientation of CFRP. The performance of the models was evaluated in terms of load carrying capacity, ductility, stiffness degradation, energy dissipation capacity and first crack load. After analysis the models, it could be concluded that CFRP is an effective material for retrofitting a beam column joint since it helped in improving the load carrying capacity, ductility, energy dissipation capacity and stiffness degradation of all the retrofitted beam column joints.

8.3 GENERAL CONCLUSIONS

The general conclusions obtained after the analysis of all the retrofitted models and normal joint are as follows: -

- Numerical model has been validated with the published test data based on experiment conducted by Mahmoud et al. (2014).
- As the number of layers of CFRP sheet increases, the load carrying capacity of the joint also increases. All three cases of alternate fiber orientation performed better than unidirectional fibers in terms of load carrying capacity.

- The failure of the retrofitted specimens shifted from columns to beams due to the strengthening of beam-column joints.
- The increase in ultimate load and deformation capacity was proportional to the number of layers of CFRP.
- The hysteretic curves of all retrofitted models were differed significantly in the push and pull directions. From the analysis of hysteresis curves, it was observed that ultimate loads and deformation capacities for models retrofitted with CFRP were significantly higher than normal beam column joint. This was primarily due to the increased joint confinement caused by externally bonded CFRP sheets.
- The increase in ultimate load and deformation capacity for retrofitted specimens with three layered CFRP with unidirectional fibers was greater than for those with two layers and one layer. The three-layered CFRP with fibers oriented at 0° and 90° had the highest stiffness and strength capacity in both positive and negative loading.
- In the case of different CFRP sheet orientations, the retrofitted model with an X-shaped sheet orientation performed slightly better than the model with an L-shaped sheet orientation.
- The use of CFRP sheets increased the ductility of all retrofitted models when compared to a standard beam column joint. Retrofitted models with three layered CFRP showed the greatest improvement in ductility in both cases of unidirectional fibers and fibers oriented at 0° and 90°.
- All of the retrofitted models outperformed the standard beam column joint in terms of energy dissipation, demonstrating that the rehabilitation strategy is effective. X shaped sheets have higher stiffness than L shaped and C shaped CFRP sheets.
- The CFRP composite acted as a very effective confinement and prevented the formation of main cracks to the joint-column region, thus stabilized reduction in secant stiffness values. Retrofitting using the proposed CFRP system dissipated more energy than the normal joint when subjected to large lateral displacements of other structural members, ensuring the structure's safety.

8.4 SPECIFIC CONCLUSIONS

The specific conclusions from the non-linear static analysis of the performance of various retrofitted models are as follows: -

- The retrofitted model with three layers of CFRP sheets performed better in terms of load carrying capacity in both cases of unidirectional fibers and fibers oriented at 0° and 90°. The improvement in the load carrying capacity of retrofitted beam column joint with 1, 2, and 3 layers of CFRP having unidirectional fibers were 18%, 42% and 55 % higher than that of the normal beam column joint.
- The load carrying capacity of retrofitted beam column joints with 1, 2, and 3 layers of CFRP with fibers oriented at 0° and 90° were 24%, 55%, and 89% higher than that of the standard beam column joint, respectively.
- The X-shaped sheet had a higher load carrying capacity than the L-shaped and C-shaped orientation. The load carrying capacity of the C-shaped orientation sheet was the lowest. The load carrying capacity of retrofitted beam column joints with X shape, L shape, and C shape CFRP sheet were 83%, 62%, and 43% higher than that of the standard beam column joint, respectively.
- In the case of models with different orientations, the X shaped sheet had the highest first crack load of 34.27 kN and the corresponding drift ratio was 2.93 %, while the C shaped sheet had the lowest first crack load with a value of 24.37 kN.
- In the case of a joint retrofitted with unidirectional CFRP fibers, the retrofitted specimen with three layers had the highest ductility among its group. The ductility of retrofitted beam column joints with 1, 2, and 3 layers of CFRP with unidirectional fibers were 64%, 81%, and 90% higher than that of the normal beam column joint, respectively.
- The ductility of 1,2, and 3 layers of CFRP retrofitted model with fibers oriented at 0° and 90° were 76%, 83%, and 92% higher than that of the normal beam column joint, respectively.
- The X-shaped sheets produced the best joint performance in terms of strength and ductility. In the case of models retrofitted with different orientations of CFRP, the ductility of retrofitted beam column joints with C shape, L shape, and X shape sheet of CFRP was 22%, 46%, and 58% higher than that of the normal beam column joint, respectively.

- The improvement in the initial stiffness of retrofitted beam column joint with 1, 2, and 3 layers of CFRP sheets with unidirectional fibers were 29%, 35% and 50% higher than that of the normal beam column joint. The improvement in the initial stiffness of retrofitted beam column joint with 1, 2, and 3 layers of CFRP with fibers oriented at 0° and 90° were 57%, 95% and 125 % higher than that of the normal beam column joint. The improvement in the initial stiffness of retrofitted beam column joint X shape, C shape, and L shape CFRP sheet were 15%, 25% and 35 % higher than that of the normal beam column joint.
- At a drift ratio of 4.5 %, the improvement in energy dissipation for three layers of CFRP sheets with unidirectional fibers was 11%, and 12% higher than for two layers and one layer. At a drift ratio of 4.4 %, three-layered CFRP sheets with fibers oriented at 0° and 90° dissipated 10% and 15% more energy than two-layered and one-layered retrofitted joints, respectively. At a drift ratio of 4.6 %, the X-shaped sheet dissipated more energy than the L-shaped and C-shaped sheets by 19% and 13%, respectively.

8.5 SCOPE FOR FUTURE STUDY

Present study is only confined to exterior beam column joint. The study can be extended to corner beam-column joints and interior beam-column joints. The present study is based on retrofitting of beam column joint using CFRP sheets in a scaled model of beam column joint. Further studies could be conducted on different retrofitting techniques like Glass Fiber Reinforced Polymer (GFRP), Aramid Fiber Reinforced Polymer (AFRP) and Basalt Fiber Reinforced Polymer (BFRP). Also, nonlinear dynamic analysis of joints could also be studied. Further studies on finding the best orientation suitable for real cases of retrofitting could also be considered.

.

REFERNCES

1. AbuTahnat, Y. B., Dwaikat, M. M. S., and Samaaneh, M. A. (2018). “Effect of using CFRP wraps on the strength and ductility behaviors of exterior reinforced concrete joint.” *Composite Structures,* , Elsevier, 20(1), 721–739.
2. ACI 318M-11 (2011), “Building Code Requirements for Structural Concrete and Commentary”, Reported by ACI Committee 318, American Concrete Institute, Farmington Hills, Michigan.
3. ACI 352R-02 (2002), “Recommendations for Design of Beam-Column Connections in Monolithic Reinforced Concrete Structures”, Reported by Joint ACI-ASCE Committee 352, American Concrete Institute, Farmington Hills, Michigan.
4. Akhlaghi, A., and Mostofinejad, D. (2020). “Experimental and analytical assessment of different anchorage systems used for CFRP flexurally retrofitted exterior RC beam-column connections.” *Structures,* Elsevier, 28(7), 881–893.
5. Al-Rousan, R. Z., Alhassan, M. A., and Al-omary, R. J. (2021). “Response of interior beam-column connections integrated with various schemes of CFRP composites.” *Case Studies in Construction Materials,* Elsevier Ltd., 14, 00488.
6. Al-Rousan, R. Z., and Alkhawaldeh, A. (2021). “Numerical simulation of the influence of bond strength degradation on the behavior of reinforced concrete beam-column joints externally strengthened with FRP sheets.” *Case Studies in Construction Materials,* Elsevier Ltd, 15(8), 00567.
7. Alsayed, S. H., Almusallam, T. H., Al-Salloum, Y. A., and Siddiqui, N. A. (2010). “Seismic Rehabilitation of Corner RC Beam-Column Joints Using CFRP Composites.” *Journal of Composites for Construction*, 14(6), 681–692.
8. Bossio, S., Antonio, F., Lignola J., Gian, P., and Andrea, M. (2017). “Design Oriented Model for the Assessment of T-Shaped Beam-Column Joints in Reinforced Concrete Frames.” *Buildings*, 7(4), 118-125.
9. Dalalbashi, A., Eslami, A., and Ronagh, H.R.(2012). “Plastic hinge relocation in RC joints as an alternative method of retrofitting using FRP.”*Composite Structures,* Elsevier Ltd, 94(8), 2433-2439.
10. Elmasry M. I. S., Abdelkader A. M., Elkordy E. A. (2018). “An Analytical Study of Improving Beam-Column Joints Behaviour Under Earthquakes”, *Sustainable Civil Infrastructures*, 65(9), 487-500.

11. Elsanadedy, H. M., Al-Salloum, Y. A., Alrubaidi, M. A., Almusallam, T. H., Siddiqui, N. A., and Abbas, H. (2021). "Upgrading of precast RC beam-column joints using innovative FRP/steel hybrid technique for progressive collapse prevention." *Construction and Building Materials*, Elsevier Ltd, 268(32), 121130.
12. Esmaeeli, E., Barros, J. A. O., Sena-Cruz, J., Fasan, L., Li Prizzi, F. R., Melo, J., and Varum, H. (2015). "Retrofitting of interior RC beam-column joints using CFRP strengthened SHCC: Cast-in-place solution." *Composite Structures*, Elsevier Ltd, 122, 456–467.
13. Fang, Y., Chen, M., and Jinlong, P.(2019). "Experimental study on seismic behaviours of hybrid FRP–steel-reinforced ECC–concrete composite columns."*Composites Part B: Engineering*, Elsevier Ltd, 176(11), 1359-8368.
14. Ganesan N., Indira P. V., Abraham R. (2007). "Steel fibre reinforced high performanceconcrete beam-column joints subjected to cyclic loading." *ISET Journal of Earthquake Technology*, 44(5), 445-456.
15. Ha, G. J., Cho, C. G., Kang, H. W., and Feo, L. (2013). "Seismic improvement of RC beam-column joints using hexagonal CFRP bars combined with CFRP sheets." *Composite Structures*, Elsevier Ltd, 95, 464–470.
16. Hadi, M. N. S., and Tran, T. M. (2014). "Retrofitting nonseismically detailed exterior beam-column joints using concrete covers together with CFRP jacket." *Construction and Building Materials*, Elsevier Ltd, 63, 161–173.
17. Hashemi, M., and Hossein, T. R.(2022). "Seismic performance of reinforced concrete beam-column joints strengthened with NSM steel bars and NSM CFRP strips." *Structures*, Elsevier Ltd, 39(6), 57-69,
18. Ilia, E., and Mostofinejad, D. (2019). "Seismic retrofit of reinforced concrete strong beam–weak column joints using EBROG method combined with CFRP anchorage system." *Engineering Structures*, Elsevier, 194(January), 300–319.
19. Kadarningsih, R., Satyarno, I., Muslikh, and Triwiyono, A. (2014). "Proposals of beam column joint reinforcement in reinforced concrete moment resisting frame: A literature review study." *Procedia Engineering*, Elsevier B.V., 95(12), 158–171.
20. Kianosh, F., Farhang, F., and Maryam, F. N., "Hysteresis behavior of 3D RC exterior beam-column joints strengthened with CFRP sheets and spike anchors." *Structures*, Elsevier Ltd, 40(8), 1065-1077.

21. Kotsouvou G., and Mouzakis H. (2012). “Exterior RC Beam-Column Joints: New Design Approach”, *Engineering Structures*, Elsevier Ltd, 41(7), 307-319.
22. Jiajia, Li., and Zhao, Y. (2019). “Double shear test on bonding mechanical properties of sprayed FRP and concrete substrate.” *Composites Part B: Engineering*, Elsevier Ltd, 162(2), 388-396,
23. Le-Trung, K., Lee, K., Lee, J., Lee, D. H., and Woo, S. (2010). “Experimental study of RC beam-column joints strengthened using CFRP composites.” *Composites Part B: Engineering*, Elsevier Ltd, 41(1), 76–85.
24. Lee, W. T., Chiou, Y. J., and Shih, M. H. (2010). “Reinforced concrete beam-column joint strengthened with carbon fiber reinforced polymer.” *Composite Structures*, Elsevier Ltd, 92(1), 48–60.
25. Mahmoud, M. H., Afefy, H. M., Kassem, N. M., and Fawzy, T. M. (2014). “Strengthening of defected beam-column joints using CFRP.” *Journal of Advanced Research*, Cairo University, 5(1), 67–77.
26. Mirza O., and Uy B. (2010). “Finite Element Analysis of the Behaviour of Composite Beam-to-Column Connections Subjected To Seismic Loading.” *Structures Congress*, 3431-3442.
27. Mostofinejad, D., and Hajrasouliha, M. (2019). “3D beam–column corner joints retrofitted with X-shaped FRP sheets attached via the EBROG technique.” *Engineering Structures*, Elsevier, 183(24), 987–998.
28. Mostofinejad, D., Shameli, S. M., and Hosseini, A. (2014). “EBROG and EBRIG methods for strengthening of RC beams by FRP sheets.” *European Journal of Environmental and Civil Engineering*, Taylor & Francis, 18(6), 652–668.
29. Faisal, M. M., and Rayhan, M. F. (2018). “A review of test methods for studying the FRP-concrete interfacial bond behavior.” *Construction and Building Materials*, Elsevier Ltd, 169(7), 877-887,
30. Najafgholipour M. A., Dehghan S.M., Dooshabi ., and Niroomandi A. (2017). “Finite element analysis of reinforced concrete beam column connections with governing joint shear failure mode.”*Latin American journal of solids and structures*, 14(4), 1200-1225.
31. Obaidat, Y. T., Abu-Farsakh, G. A. F. R., and Ashteyat, A. M. (2019). “Retrofitting of partially damaged reinforced concrete beam-column joints using various plate-configurations of CFRP under cyclic loading.” *Construction*

and Building Materials, Elsevier Ltd, 198, 313–322.

32. Ong, C., Chau-Khun, M., Jia-Yang, T., Abdullah, Z. A., and Wahid, O. (2022). "Seismic retrofit of reinforced concrete beam-column joints using various confinement techniques: A review." *Structures*, Elsevier Ltd, 42(2), Pages 221-243.
33. Panjwani, P., and Dubey, D. S. K. (2015). "Study of Reinforced Concrete Beam-Column Joint." *International Journal of Engineering Research*, 4(6), 321–324.
34. Patil S. S., and Manekari S. S. (2013). "Analysis of Reinforced Beam-Column Joint Subjected to Monotonic Loading." *International Journal of Engineering and Innovative Technology*, 2 (10), 149-158.
35. Pohoryles, D. A., Melo, J., Rossetto, T., D'Ayala, D., and Varum, H. (2018). "Experimental Comparison of Novel CFRP Retrofit Schemes for Realistic Full-Scale RC Beam–Column Joints." *Journal of Composites for Construction*, Elsevier Ltd, 22(5), 04018027.
36. Prasanna K., Ramasubramani R., Anandh K. S., Saisabarish, and Maddu V. K. (2017)."Strengthening of Beam-Column Joint With Steel Fibre Reinforced Concrete Under Seismic Loading."*Earth and Environmental Science*, 80(2), 1-11.
37. Roberto, R., Annalisa, N., Joaquín, G., and Ruiz, P.(2014). "Cyclic behavior of RC beam-column joints strengthened with FRP systems." *Construction and Building Materials*, Elsevier Ltd, 54, 282-297.
38. Rodríguez, V., Guerrero, H., Alcocer, S. M., and Tapia-Hernández, E. (2021). "Rehabilitation of heavily damaged beam-column connections with CFRP wrapping and SFRM casing." *Soil Dynamics and Earthquake Engineering*, 145(March).
39. Sarkar P., Agrawal R., and Menon, D. (2007). "Design of RC Beam-Column Joints Under Seismic Loading- A Review", *Journal of Structural Engineering*, 33(6), 449-457.
40. Seyed, S. M., and Hamid, R. R.(2010). "Strength and ductility of FRP web-bonded RC beams for the assessment of retrofitted beam–column joints."*Composite Structures*, Elsevier Ltd, 92(6), 1325-1332.
41. Sharma, R., and Bansal, P. P. (2019). "Behavior of RC exterior beam column joint retrofitted using UHP-HFRC." *Construction and Building Materials*,

Elsevier Ltd, 195, 376–389.

42. Shang, X., Lu, Z., Yu, J. (2016).“Efficiency of externally bonded L-shaped FRP laminates in strengthening reinforced-concrete interior beam-column joints.” *Composite Structures*, Elsevier Ltd, 20, 434-455.
43. Sheela S., and Geetha B. A. (2012). “Studies on the Performance of RC Beam-Column Joints Strengthened Using Different Composite Materials.”*Journal of Infrastructures Engineering*, 93(7), 63-71.
44. Singh, V., Bansal, P. P., Kumar, M., and Kaushik, S. K. (2014). “Experimental studies on strength and ductility of CFRP jacketed reinforced concrete beam-column joints.” *Construction and Building Materials*, Elsevier Ltd, 55, 194–201.
45. Uma S. R., Jain S. K. (2006). “Seismic design of beam-column joints in RC moment resisting frames – Review of codes”, *Structural Engineering and mechanics*, Vol. 23(5), 579-597.
46. Uma, S. R., and Prasad. (2015). “Seismic Behavior of Beam Column Joints in Reinforced Concrete Moment Resisting Frames.” *Earthquake*, 2(7), 1–36.
47. Unal, M., and Burak, B. (2013). “Performance of Beam-to-Column Connection of a Well-Detailed RC Moment Frame Building under Pseudo-dynamic Loading.” *Journal of Structural Engineering*, 139(6), 886-896.
48. Venkatesan, B., Ilangovan, R., Jayabalan, P., Mahendran, N., and Sakthieswaran, N.(2016). “Finite element analysis (FEA) for the beam-column joint subjected to cyclic loading was performed using ANSYS.”*Scientific Research Publishing*, 7(8), 1581-1597.
49. Wang, G. L., Dai, J. G., and Bai, Y. L. (2019). “Seismic retrofit of exterior RC beam-column joints with bonded CFRP reinforcement: An experimental study.” *Composite Structures*, Elsevier Ltd, 224, 111018.
50. Yalçin, C., Kaya, O., Biçer, E., and Parvin, A. (2019). “Retrofitting of reinforced concrete beam-column joints by composites-part II: Analytical study.” *ACI Structural Journal*, 116(1), 31–40.

LIST OF PUBLICATIONS

Seena, J., Ambi, R. (2022). "Numerical Analysis of Reinforced Concrete Beam Column Joint retrofitted using Carbon Fiber Reinforced Polymer (CFRP) sheets." Proceedings of International Virtual Conference on "*Emerging Research Trends in Structural Engineering (ERTSE 2022)*", Organized by School of Civil Engineering, Vellore Institute of Technology (VIT), Chennai.